# DOUBLE SAMPLING FOR COARSE WOODY DEBRIS ESTIMATIONS FOLLOWING LINE INTERSECT SAMPLING

By
Allissa Lane Corrow

B.S. Western Washington University, Bellingham, Washington, 2007

Thesis

presented in partial fulfillment of the requirements
for the degree of

Master of Science
Resource Conservation

The University of Montana
Missoula, MT

May 2010

Approved by:

Perry Brown, Associate Provost for Graduate Education
Graduate School

Dr. David L.R. Affleck, Chair
Department of Forest Management

Dr. Elizabeth Dodson
Department of Forest Management

Dr. David Patterson
Department of Mathematical Sciences

Double sampling for coarse woody debris estimations following line intersect sampling

Chairperson: Dr. David L.R. Affleck

Coarse woody debris (CWD), an essential component of healthy forests, has typically been defined as dead and down, large woody material. Quantification of this resource provides a useful metric for assessing wildlife habitat, fuel loading, and more recently, carbon sequestration. Although many CWD sampling methods exist, accurate estimation is difficult and expensive. Double sampling incorporates auxiliary data that is positively correlated with the attribute of interest as a means of reducing sampling costs and/or increasing estimation precision. The present study investigated double sampling applications to the common CWD sampling technique, line intersect sampling (LIS). We identified aggregate length as a potential auxiliary variable for estimating aggregate volume and abundance of CWD. However, further analysis indicated that the cost difference of the sampling phases, coupled with the correlation of the variables was not sufficient to warrant double sampling in the study area. Further investigation is needed to develop accurate and efficient CWD sampling methods with widespread applicability.

# ACKNOWLEDGEMENTS

I would like to thank my advisor, Dr. David. L.R. Affleck, for taking my basic knowledge of statistics and transforming it into a workable skill set. If it weren't for your patience and countless explanations of statistical theory and sampling designs, I would not be here today. Thanks to my committee members Dr. David Patterson and Dr. Elizabeth Dodson for their comments, flexibility and patience during this arduous process. Also thanks to the College of Forestry and Conservation and the McIntire-Stennis USDA Cooperative Forestry Grant for project funding. Without this support I would be eternally bound to student debt, rather than just temporarily.

Thanks to the Rocky Mountain Research Station, especially Rachel Loehman and Emily Heyerdahl, for providing me with an incredible opportunity to apply my degree and retire my pulaski.

A special thanks to my fellow grad students, especially Heath Carey, Angela Meyer, Kyla Zaret, Emily Garlough, Alan Swanson, Katie Jorgenson, Chris Carlson, Dylan Boyle and Aaron Flesch for support, comic relief, and technical assistance. Your friendship has kept me sane and your inspiration has pulled me through.

And finally, my sincerest thanks to my family. Mom, without your unfaltering guidance and support I would have given up long ago. Grandma, thanks for always believing in me and for providing a willing ear. Maggie, you challenge me to be my best and call me out when I need it- thank you. Yvonne, your confidence has inspired me to rise to the challenge time and time again. Keep up the hard work and you'll be here very soon too.

To everyone that helped me in these last two years- Thank you, thank you, thank you!

# TABLE OF CONTENTS

TABLE OF CONTENTS (continued)

# LIST OF TABLES

# LIST OF FIGURES

# LIST OF NOTATION

| Notation | Units | Definition |
|---|---|---|
| $L$ | m | Segment length |
| $n$ | | Sample particle count |
| $A$ | ha | Stand area |
| $K$ | | Number of sample points |
| $\pi_i$ | | Inclusion probability of the $i$th particle |
| $l_i$ | m | Horizontal length of the $i$th particle |
| $s_i$ | m | Slope length of the $i$th particle |
| $p_i$ | % | Percent tilt of the central axis of the $i$th particle |
| $q_i$ | | Number of lobes of the $i$th particle |
| $D_{ij}$ | cm | Diameter of the $j$th lobe of the $i$th particle |
| $\hat{v}_i$ | $m^3$ | Estimated volume of the $i$th particle |
| $M$ | | Number of segments in a stand |
| $M_t$ | | Number of timed segments in a stand |
| $G$ | $m \cdot ha^{-1}$ | Aggregate length of CWD per unit area |
| $\hat{G}_k$ | $m \cdot ha^{-1}$ | Estimated $G$ from point $k$ |
| $\bar{G}$ | $m \cdot ha^{-1}$ | Mean of $K$ point estimates of $\hat{G}_k$ |
| $s_{\hat{G}}$ | $m \cdot ha^{-1}$ | Estimated standard deviation of point estimate $\hat{G}_k$ |
| $CV_{\hat{G}}$ | % | Coefficient of variation of point estimate $\hat{G}_k$ |
| $V$ | $m^3 \cdot ha^{-1}$ | Aggregate volume of CWD per unit area |
| $\hat{V}_k$ | $m^3 \cdot ha^{-1}$ | Estimated $G$ from point $k$ |
| $\bar{V}$ | $m^3 \cdot ha^{-1}$ | Mean of $K$ point estimates of $\hat{V}_k$ |
| $s_{\hat{V}}$ | $m^3 \cdot ha^{-1}$ | Estimated standard deviation of point estimate $\hat{V}_k$ |
| $CV_{\hat{V}}$ | % | Coefficient of variation of point estimate $\hat{V}_k$ |
| $N$ | $\# \cdot ha^{-1}$ | Abundance of CWD per unit area |
| $\hat{N}_k$ | $\# \cdot ha^{-1}$ | Estimated $N$ from point $k$ |
| $\bar{N}$ | $\# \cdot ha^{-1}$ | Mean of $K$ point estimates of $\hat{N}_k$ |
| $s_{\hat{N}}$ | $\# \cdot ha^{-1}$ | Estimated standard deviation of point estimate $\hat{N}_k$ |
| $CV_{\hat{N}}$ | % | Coefficient of variation of point estimate $\hat{N}_k$ |

# LIST OF NOTATION (continued)

| Notation | Units | Definition |
|---|---|---|
| $\rho$ | | Population correlation coefficient |
| $r_p$ | | Sample Pearson correlation coefficient |
| $r_{MCD}$ | | Sample MCD correlation coefficient |
| $t_c$ | min | Count time; phase 1 sample time |
| $t_t$ | min | Total time; phase 2 sample time |
| $t_{km}$ | min | Sample time at point $k$ segment $m$ |
| $f$ | | Optimal sample size ratio |
| $\hat{a}$ | | Slope of the least squares regression line |
| $\hat{b}$ | | Intercept of the least squares regression line |
| $e$ | | Error term associated with the regression |
| $s_e$ | | Standard error of the regression residual |
| $\bar{n}_t$ | | Mean number of particles from timed segments |
| $\bar{n}$ | | Mean number of particles from all segments in a stand |

# 1. INTRODUCTION

## *1.1 Ecological Roles of CWD*

Coarse woody debris (CWD) plays an integral role in ecosystem processes and forest structure. It provides habitat for plants, animal and microbes, contributes fuel to wildfires, and returns valuable nutrients to the soil through decomposition. CWD also sequesters carbon and may serve as an important sink of global carbon. A recent inventory estimates that 14% of temperate forest carbon is contained in dead woody material, 34% in live vegetation and 52% in the soil (Woodall *et al*. 2008). The influx and persistence of CWD is largely attributed to natural and human caused disturbance events, as well as climatic conditions (Woodall & Liknes 2008). The importance of this resource and the evidence of global climate change make accurate estimation of CWD attributes essential for effective forest management.

CWD is a highly dynamic resource that is largely dependent on land management activities and natural disturbance (Harmon *et al.* 1986). CWD input has been closely related to rates of tree mortality, in some cases (Brown 2002; Franklin *et al*. 1987). However, tree mortality is not constant, and depends on a multitude of factors, such as stand age and productivity (Franklin *et al*. 1987), insect and disease outbreak (Klutsch *et al*. 2009; Ulyshen *et al*. 2004), and disturbance (Harmon *et al*. 1986). Events such as logging, wildfire and windthrow can create large amounts of CWD in a short period.

CWD persistence is largely dependent on climatic conditions (i.e. temperature and moisture; Woodall & Liknes 2008) and disturbance events (Monsanto & Agee 2008). It has also been a concern that site disturbance during sampling efforts alters the decomposition rate of CWD, especially fine fuels (Woodall *et al.* 2008). Decomposition rates increase with temperature and moisture (Harmon *et al*. 1986; Spetich *et al*. 1999), and with the global change in climate patterns expected, one can only speculate that CWD decomposition rates will be affected (Woodall & Liknes 2008). Therefore, accurate estimations are crucial for detecting changes in the amount and persistence of CWD over time.

## *1.2 CWD Attributes*

The utility of CWD is measured by various attributes. Often, when a particle is sampled, diameter, length, species, decay class, tilt, and orientation are measured. From these variables, population attributes such as aggregate length, volume, biomass, and abundance can be estimated. In many CWD inventories, volume is of primary interest. Volume provides a useful metric for site comparison, fuel loading, and habitat geomorphology.

### 1.2.1 Abundance and Volume

Wildlife biologists are often interested in CWD abundance (*e.g.* MacNally *et al.* 2001; Stevenson *et al*. 2006) and volume as CWD provides shelter, nesting habitat, travel corridors or foraging habitat for nearly all types of wildlife (Harmon *et al.* 1986; Stevens 1997). Species of birds (Bull & Holthausen 1993; Hutto 1995, 2006), mammals (Bowman *et al.* 2000; Carey & Johnson 1995; Manning & Chytyk 2008; McCay 2000), amphibians (McKenny *et al*. 2006; Todd *et al.* 2009), and reptiles (Owens *et al.* 2008) all benefit from various amounts and distributions of CWD (Harmon *et al*. 1986; Stevens 1997). A study of the pileated woodpecker (*Dryocopus pileatus*) in Oregon, observed foraging on downed logs 38% of the time, and recommended CWD retention as a management objective for habitat conservation. Large furbearing mammals benefit indirectly by preying on small mammals and birds that depend on CWD (Manning & Chytyk 2008). Moisture and temperature sensitive animals, such as reptiles and amphibians, depend on the structural diversity and microhabitat provided by CWD (Owens *et al*. 2008). Indeed the species richness of a site is positively correlated with the relative abundance and availability of CWD (Zielonka & Piatek 2004). In Sweden, 26% of red-listed species depend on downed logs, while another 21% depend on standing snags (Ringvall & Stahl 1999). Aside from the abundance and volume of CWD, many wildlife species select habitat sites according to various qualitative CWD characteristics, including whether the material is standing or downed, its species, and its decay status.

CWD volume is also of interest to fire managers in terms of fuel loading (Woodall *et al*. 2005; Sikkink & Keane 2008). The composition of surface fuels affects fire intensity and burn severity (Agee 1993). Continuity of surface fuels, fine fuels and CWD, can determine if a flaming front will carry across the landscape (Reinhardt *et al.*

1997) and largely affects post fire soil characteristics (Metzger *et al*. 2008). Small woody and fine fuels increase the intensity, given the right weather and moisture conditions (Brown *et al*. 2003), but CWD contributes more to severity than intensity (Agee 1993). In contrast to the quick and short-lived ignition of fine fuels, CWD ignites slowly through smoldering combustion and retains heat for a much longer duration (Albini & Reinhardt 1995). The close proximity of downed logs to the soil means that radiant and conductive heat projects downwards potentially causing extreme soil heating (Brown *et al.* 2003). Fine root and vegetative cell death can occur when soil temperatures reach 60 degrees Celsius for a minute or more (Agee 1993; Albini & Reinhardt 1995) and as the soil temperature nears 200°C, a hydrophobic layer may form, increasing erosion potential (Monsanto & Agee 2008). Soil hydrophobicity is especially common in forests with a high proportion of waxy or resinous foliage (Agee 1993), such as the conifer forests of western Montana.

Simply put, the post-fire conditions are directly influenced by the available fuels. Fire managers hoping to achieve a specific burn objective will benefit from accurate estimates of surface fuels. Wildfire risk is mitigated by actively treating and monitoring forested areas to meet fuel loading guidelines and protocols. CWD is an important component of forest fuels, and accurate fuel load measurements are essential for effective fuel management (Sikkink & Keane 2008).

### 1.2.2 Decay and CWD Dynamics

The combustibility of CWD is a function of its stage of decomposition as well as its species-specific density properties. Post fire studies have shown that a disproportionate amount of decayed wood (decay class 3, 4 &0 5; *e.g*. Harmon *et al*. 1986) is consumed, relative to sound wood (decay class 1 & 2). In Montana, for example, 85% of decayed CWD was consumed during a prescribed fire, relative to only 36% of sound CWD consumption (Rogers & Steele 1980). Similar results have been found after under-burning in Arizona (Covington & Sackett 1984) and after a wildfire in Yellowstone National Park (Tinker & Knight 2000).

Combustion of CWD, be it decayed or sound, effectively converts forest carbon sinks into sources, and has been recognized for its substantial contribution of atmospheric $CO_2$ (Kashien *et al*. 2006; Woodall *et al*. 2008). CWD input and decay creates a constant

ebb and flow of forest carbon stocks (Harmon *et al.* 1986). As attention focuses on monitoring carbon fluxes worldwide, it is important to consider the role of CWD in the global system (Woldendorp *et al.* 2004). In North American forests, coarse and fine woody debris are more abundant and more persistent at higher latitudes than lower latitudes (Woodall & Liknes 2008). Considering that decomposition rates generally increase with temperature and moisture (Keane 2008a), climate change may put substantial carbon stocks at risk (Woodall & Liknes 2008) creating a feed-forward mechanism for further change.

Decomposition is a natural process, however, and an important component of ecosystem function. As material decays, carbon is released into the atmosphere as carbon dioxide (Keane 2008a), and essential nutrients are returned to the soil and made available for plant regeneration (Harmon *et al.* 1986). Inasmuch as plants depend on CWD decomposition, wildlife species require CWD at various stages of decay. As CWD decomposes the suite of species utilizing the material changes (Thomas 1979). Some highly specialized species occur exclusively in areas containing CWD particles of a specific size or decay class (Hutto 2006; Thomas 1979). Structurally sound logs serve as travel ways across barriers and as elevated lookouts and perches (Harmon *et al.* 1989; Thomas 1979). As decay softens the material, loose bark and cracks provide hiding spaces and thermal cover. As small mammals burrow into logs, fragmentation ensues (Bowman *et al.* 2000), exposing the internal material for amphibian and reptile foraging. For example, the abundance of red-backed salamanders (*Plethodon cinereus*) is positively related to the abundance of well decayed, downed CWD, and negatively correlated to that of poorly decayed CWD (McKenny 2006). During later stages of decay, microbes, invertebrates and fungi concentrate in the centers of the particles (Keane 2008b), which aid the further breakdown of CWD into soil organic matter.

The dynamic nature of CWD affirms the need for accurate and frequent measurements of this valuable resource. Following the agreement signed at the 1992 United Nations Framework Convention on Climate Change, the US and 150 other nations are now working to implement inventory programs of forest carbon stocks (Woodall *et al*. 2008). Accurate baseline carbon stock data is essential for tracking changes as climate regimes change. However, despite the importance of such data, some US states still have

little to no CWD measurements reported (Woodall *et al*. 2008). Furthermore, of the 150+ countries that signed the 1992 agreement, very few have implemented a nationwide inventory program for CWD (Woodall *et al.* 2008). This lack of follow-through, both in the US and globally, indicates a need to identify and address problems associated with current CWD sampling strategies.

## *1.3 CWD Sampling Strategies*

### 1.3.1 Line Intersect Sampling

Many CWD sampling methods have been devised, with variable success in terms of the implementation ease and accuracy of attribute estimation. Line intersect sampling (LIS) (also referred to as planar, Brown's transect, and line intercept sampling) is a common CWD sampling method (Woodall *et al.* 2009) and is used extensively for estimating biomass and woody fuel volume, and other downed wood characteristics. Fore example, the US Forest Inventory and Analysis (FIA) program uses a variation of the LIS method (Woodall *et al*. 2008) to assess habitat, structural stability, forest biomass and carbon, fuel loading, and treatment effectiveness. The FIA program employs a three phase sampling approach, in which CWD is sampled during the least intensive subset.

LIS was developed by Canfield in 1941 and first applied to downed wood by Warren and Olsen in 1964 to survey logging waste in New Zealand. LIS is an unequal probability sampling design, utilizing a fixed length line transect (DeVries 1973, 1974). Particles are selected proportional to their lengths, with larger particles having a greater chance of being intersected by a fixed length transect. If the central axis of a particle is intersected by the transect segment, the particle is included in the sample. The central axis can be defined as the longest horizontal line that connects two points on the boundary of the particle (Gregoire & Valentine 2008).

Many US government agency protocols are developed based on fuel estimates acquired using a common variation of line intercept sampling (LIS), commonly referred to as "Brown's Transect" sampling (Brown 1974). Consistent with the National Fire Danger Rating System (NFDRS), woody fuels are tallied by "time lag" (TL) fuel class, which relate particle diameter to the rates at which the fuels respond to changes in moisture content (Table 1.1). CWD particles are tallied on the full transect length,

whereas smaller particles are only tallied for a subsection of the transect. For example, on FIA transects and National Park Service (NPS) fuels transects 1 hour fuels (> 0.25 inch in diameter), 10 hour fuels (0.25 to 1 inch in diameter), and 100 hour fuels (1 to 3 inches in diameter) are tallied for only a segment of the transect. Coarse woody fuels, which correspond with the 1000+ hour fuels (> 3 inches or 7.6 cm in diameter), are tallied for the entire length of the transect. Diameter measurements are used to estimate fuel volume, which is then converted to biomass expressed as Megagrams (equivalent to metric tons) per hectare ($Mg \cdot ha^{-1}$).

**Table 1.1**. Woody debris/fuels size classes and sampling distances for NPS fuel transects.

| Intersection Diameter | Fuel-hour Class (hr) | Distance to Tally Along Transect |
|---|---|---|
| 0 to 0.25 inch | 1 | 0 to 6 ft |
| 0.25 to 1 inch | 10 | 0 to 6 ft |
| 1 to 3 inches | 100 | 0 to 12 ft |
| > 3 inches | *1000 + | 0 to 50 ft |

Source: USDI National Park Service, 2001

### 1.3.2 Double Sampling

Volume estimators following LIS have high variability, and require large samples to achieve standard errors less than 50% of the mean (Woldendorp *et al*. 2004). It is thus worth enquiring whether auxiliary information or variables can be integrated into this strategy in order to improve the precision of parameter estimation. In standing tree surveys for example, if stand volume is the variable of interest, basal area can often be effectively used as an auxiliary variable for estimation, due to its strong positive correlation with volume, and relative ease with which it can be measured. Double sampling exploits this correlation at the estimation stages, using the association of the auxiliary variable and variable of interest to reduce sampling costs or improve estimation accuracy (Shiver & Borders 1996).

Double sampling (*i.e.* two phase sampling) involves two distinct sampling phases, each employing different sample sizes. In cases where field measurements are costly or time consuming, considerable savings can be made by double sampling strategies. In phase 1, measurements necessary for estimation of the auxiliary variable are obtained, and this first phase is generally allocated the bulk of the time and resources. However, once these data on the auxiliary variable are obtained, the second phase sample need only

consist of a few measurements of the variable of interest. The association between variables can then be used to derive ratio or regression estimates of the parameters of the attribute of interest (Shiver & Borders 1996; Gregoire & Valentine 2008).

Carrying forward the previous example, volume measurements on standing trees are difficult and labor intensive. Hence during a first phase, many plots are established purely for basal area estimation. Because tree volume is highly correlated with basal area, the second phase consists only of a subset of phase one plots (or an entirely new set of plots) and obtains detailed measurements for estimating tree volume (*i.e*. tree diameter, height, and taper). Regardless of whether the phase 2 plots are a subset of phase 1, or a new sample of plots, the information from the two phases can be combined to give precise estimates of stand volume.

Reductions in standard error generally can be expected when the attribute of interest is relatively costly to sample or difficult to measure accurately (Gregoire & Valentine 2008). The strength of the correlation between two variables and the cost difference between phase 1 and 2 sampling also determines the potential advantage of double sampling endeavors. The greater the difference in sampling cost, the less correlated the variables need be to justify double sampling. Likewise, the stronger the correlation, the lower the cost ratio needed between the sampling phases to make double sampling worthwhile (Shiver & Borders 1996; Fig. 1.1).

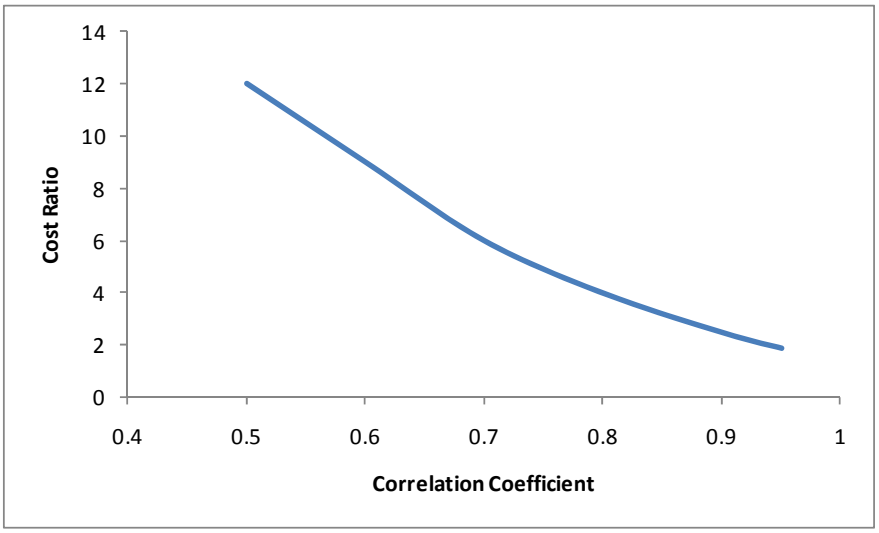


**Figure 1.1.** Correlation between a variable of interest and an auxiliary variable. For double sampling to be beneficial, the corresponding ratio of phase 2 sampling costs to phase 1 sampling costs must be exceeded (from Shiver & Borders 1996 p.212).

## ***1.4 Study Objectives***

If double sampling can be integrated into sampling strategies such as LIS, the current difficulties associated with accurate and efficient CWD inventories may be mitigated. For example, when faced with a 30% budget cut, the Swiss National Forest Inventory adopted a double sampling design to achieve the accuracy of a previous, single phase sampling design (Mandallaz & Ye 1999). Such strategies could make CWD and carbon stock assessment more feasible for agencies or individual land owners attempting to initiate programs similar to the FIA. As associated sampling costs are decreased, the number of sample locations could be increased, yielding more precise CWD inventories, and providing more reliable information for land managers, policy makers and forest stewards.

The objective of the present study was to investigate potential double sampling applications to increase efficiency and precision of CWD estimates. More specifically, we set out to:

1. Examine the variability associated with LIS estimates of CWD attributes in conifer stands in western Montana;

2. Identify useful auxiliary variable(s) for key CWD attribute estimates;

3. Investigate the efficiency of CWD attribute estimations based on two phase LIS strategies.

# 2. METHODS

## *2.1 Field Methods & Data Collection*

Field work was conducted within the Lubrecht Experimental Forest (49°54'N, 113°27'W) from June to August of 2008. Lubrecht is an 11500 hectare tract located in western Montana, approximately 50 km northeast of Missoula, at an elevation ranging from 1100 to 1900 meters above sea level (Figure 2.1).

### *2.1.1 Initial Study Set-up*

Sample locations were distributed across 7 stands with a variety of dominant and co-dominant tree species. The 4 most common tree species were ponderosa pine *(Pinus ponderosa* C. Lawson), Douglas-fir (*Pseudotsuga menziesii* Mirb. Franco), western larch (*Larix occidentalis* Nutt), and lodgepole pine (*Pinus contorta* Douglas ex. Louden). Stands were selected such that a range of forest structure and cover types would be sampled. Attributes considered included: dominant overstory species, stand age, topography, tree basal area, and CWD abundance and distribution. All of the selected stands have likely been disturbed in the past, but have since recovered to a secondary forest structure. Stand age ranged from approximately 40 to 150 years.

Prior to sampling commencement, a pilot study was conducted in each stand to roughly estimate CWD particle abundance. Segment length ($L$) was then adjusted on a per stand basis to capture approximately 9 particles per sampling point using:

$$\frac{L}{9} \approx \frac{L_P}{n_p} \quad [2.1]$$

where $L_P$ is the length of the pilot transect and $n_p$ is the number of particles encountered along the pilot transect for a given stand.

The initial intent was to sample 1-2 points per hectare in each of 9 selected stands. However, it soon became apparent that this was not a feasible workload for the given time frame. The number of stands was reduced to 7, and the number of points per stand varied as time allowed (Table 2.1)

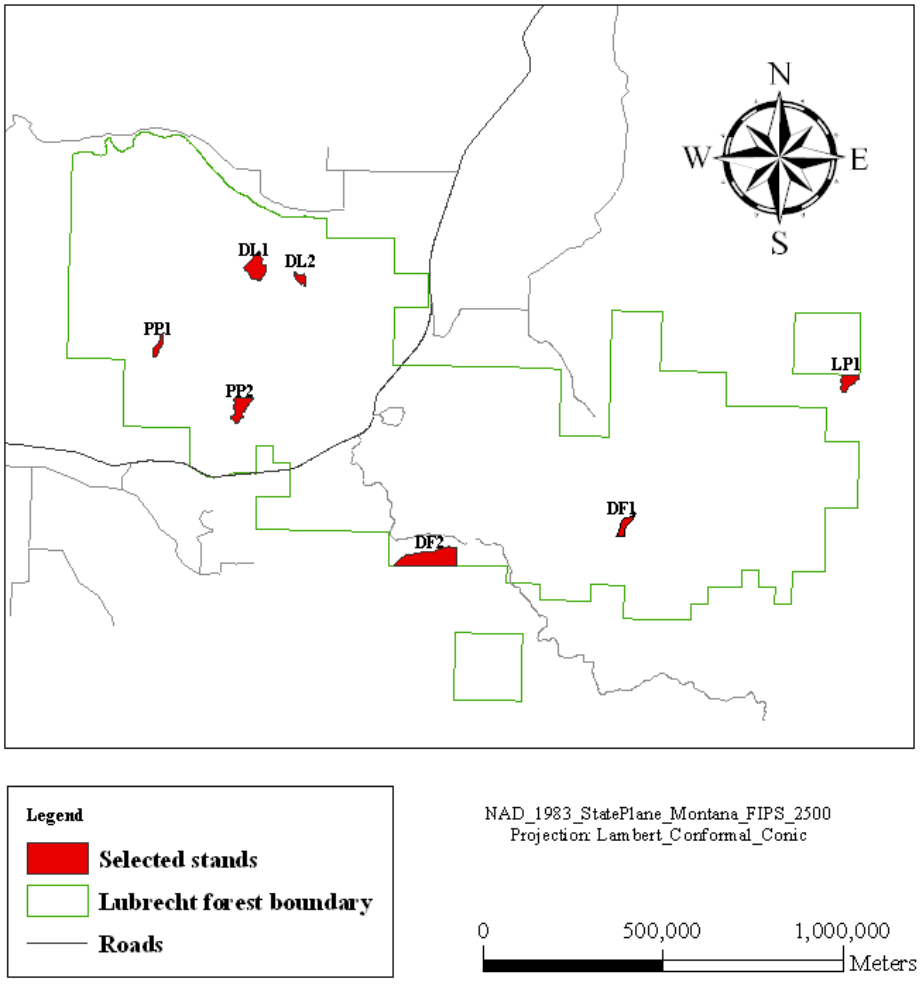


**Figure 2.1** Selected stands at Lubrecht Experimental Forest

**Table 2.1** Selected stands, area, number of LIS samples, number of basal area (BA) points, and LIS transect lengths (*L*).

| Stand | ID | Area (ha) | Sample Points | BA Points | *L* (m) |
|---|---|---|---|---|---|
| 169 | DL1 | 20.17 | 30 | 8 | 14 |
| 237 | DL2 | 10.87 | 28 | 7 | 11 |
| 413 | PP1 | 6.16 | 28 | 11 | 8 |
| 621 | PP2 | 13.87 | 30 | 8 | 50 |
| 1201 | DF1 | 7.78 | 24 | 8 | 15 |
| 1351 | DF2 | 28.6 | 60 | 10 | 16 |
| JSPL | LP1 | 11.41 | 28 | 8 | 3 |

### ***2.1.2 Stand attribute data***

At a subset of the sample points (Table 2.1), stand basal area (BA) was estimated using a 2.3 $m^2 \cdot ha^{-1}$ (equivalent to a 10 $ft^2 \cdot ac^{-1}$) BAF relascope. Sample trees were identified to species to provide a measure of species composition and dominant cover type. Additionally, travel time (min) and distance (m) to the BA sample points were recorded to provide a metric for travel efficiency in a given stand.

Stands were assigned identifiers based on dominant species relative to basal area (Table 2.1). The first letters of leading species' common names were used for the stand identifiers, followed by a sequential number (*e.g.* DF1 for Douglas-fir stand 1). Stands co-dominated by Douglas-fir and western larch were labeled DL1 and DL2. This does not imply that Douglas-fir is more abundant than western larch, rather that both species were approximately equal in abundance.

### ***2.1.3 Sample point data***

Sample point locations were selected uniformly at random throughout each of the 7 stands. At each sample location, three transect segments (A, B, and C) were laid out radiating from a central point, forming a Y shape. Orientation of segment A was selected uniformly at random and segments B and C were oriented at +/- 120 degrees of the segment A azimuth. Sampling was initiated 2 m from the sample point to disperse the sampling effort and reduce the occurrence of particles being intersected by multiple segments. This had the additional effect of reducing trampling of particles near the sampling point.

When a transect segment encountered a stand boundary, the reflection method was used to correct for edge effect (Gregoire & Monkevich 1994). The reflection method

requires that the portion of the segment that would lie outside the stand boundary be 'folded back' into the stand, so that the original transect segment is re-sampled for the remaining length of the segment. If the length of the reflected portion of the segment is greater than the in-bounds portion, the reflected portion continues beyond the segment origin, with the opposite orientation. For example, if a 30 m transect segment with orientation 90° encounters the stand boundary after 10 m, the reflected segment would retrace the first 10m and extend another 10 m in the direction of 270° past the origin.

This field work was conducted in conjunction with a separate study of the line intersect distance sampling (LIDS) method (Affleck 2008). Both methods were used at each point, utilizing a common transect origin and segment orientation, thus encountering many of the same particles in both sampling efforts. The ordering of sampling was randomized, allowing for each method to be employed first for 50% of the sample points. Both LIS and LIDS were to be examined for efficiency, thus sampling time was recorded for both methods. In order to obviate bias introduced by previous searches over the same ground, time was recorded for only the first sampling method implemented at a point. At each sample point, we first recorded the time to set up the transect segment and count the number of qualifying particles ($t_c$). Next, a separate time was recorded for particle measurements on each transect segment. This resulted in a count time and a measure time for each LIS transect segment, at 50% of the sample points. Count time was used to represent the time (or cost) required for phase 1 sampling. The combined count time and measure time ($t_t$) was used to represent the time required for phase 2 sampling.

### ***2.1.4 Particle data***

A particle of downed wood was included in the present study if:

1. any point along its length measured 7.5 cm in diameter or greater,
2. it was not attached to a living tree,
3. it was leaning at least 45 degrees from vertical,
4. its central axis was intersected by a transect segment.

Note that only the portions of a qualifying particle found within 2 m of the ground were considered (*i.e.* suspended fragments of wood were not measured).

The central axis of a particle was defined as the straight line connecting the two furthest points on the particle boundary. For straight logs, this usually corresponded with the pith. If the particle was sufficiently curved, however, the central axis could have crossed the particle boundary (Figure 2.2).

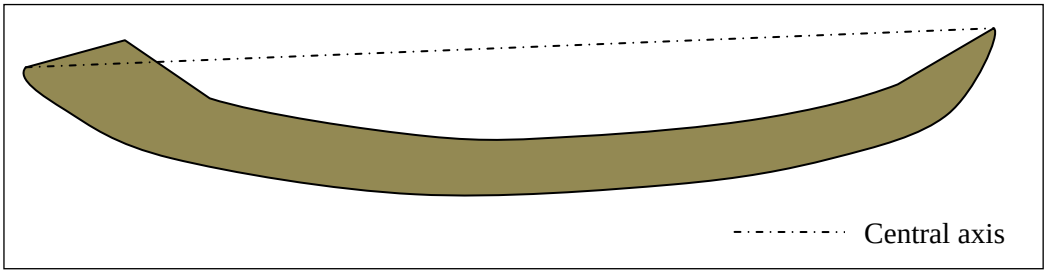


**Figure 2.2** The central axis of a curved CWD particle.

The diameters of each particle were measured with a caliper, to the nearest tenth of a centimeter. Measurements were taken in the vertical plane running perpendicular to the particle's central axis, at the intersection of the central axis and the transect segment. Two diameter measurements were taken for out-of-round particles, one horizontal and one vertical (Fig. 2.3). In cases where multiple connected lobes (*i.e.* branches) crossed the vertical plane perpendicular to the central axis, diameter measurements were taken for each of the lobes (Fig. 2.4). The length of the central axis of each particle was recorded to the nearest centimeter. The percent of particle tilt from horizontal was measured along the central axis using a clinometer.

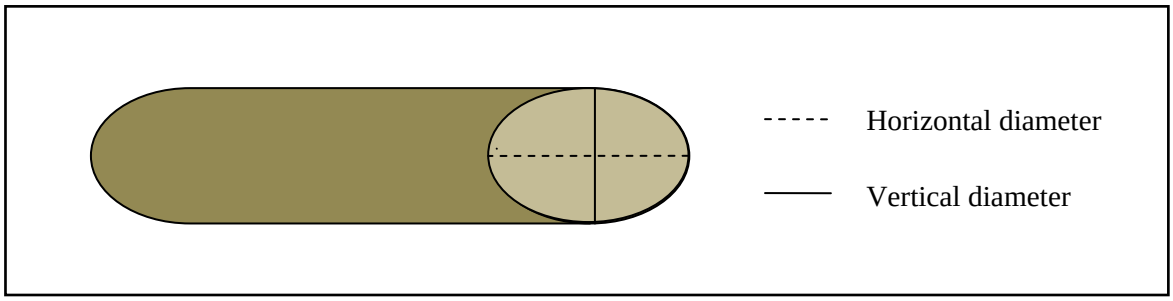


**Figure 2.3** Two diameter measurements are taken for out-of-round particles, one in the vertical plane and one in the horizontal plane, perpendicular to the central axis.

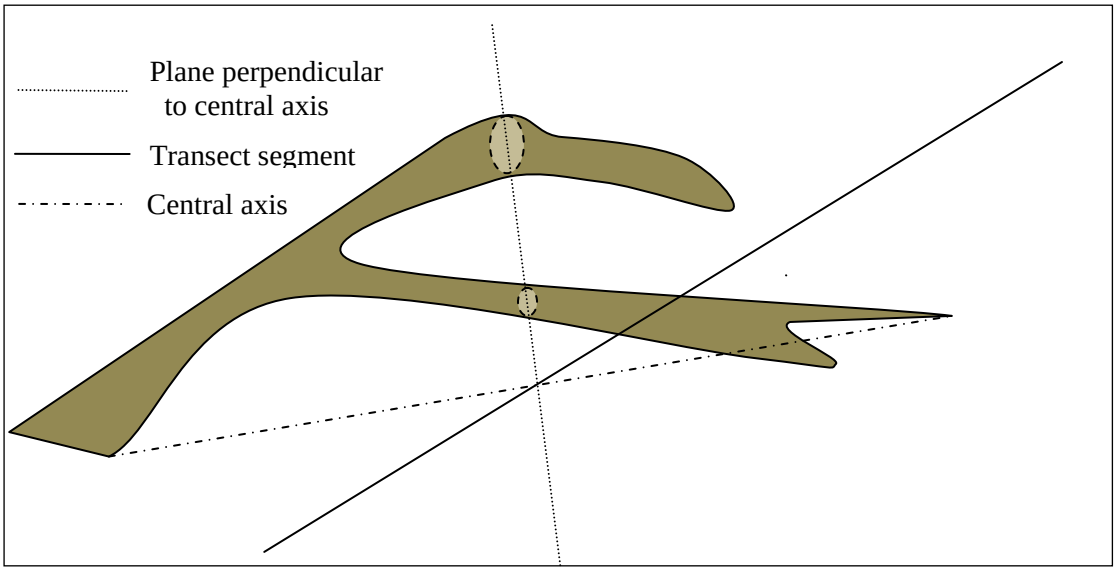


**Figure 2.4** Diameter measurements for a multiple lobed particle are taken on each cross section in the plane perpendicular to the central axis at the point of intersection with the transect segment.

Particle species was recorded as conifer, hardwood, or unknown. Particle decay class was recorded on a scale of 1-5, according to structural integrity and physical appearance (Harmon *et al.* 1986). Decay class 1 consisted of freshly fallen particles that were fully intact and retained all or most of the bark. Particles of the decay class 5 were highly decomposed and no longer held the original shape of the log.

## *2.2 Attribute Estimation*

### *2.2.1 Aggregate Length*

LIS is an unequal probability sampling design that selects particles with probabilities proportional to their lengths. Thus, long particles are more likely to be selected than short particles. When randomly oriented Y-shaped transects are used the inclusion probability $\pi_i$ of the $i$th particle is:

[2.2] $$\pi_i = 3L\frac{2l_i}{10000\pi A}$$

where $L$ is the segment length (m), $l_i$ is the horizontal length of the $i$th particle (m), $A$ is the stand area (ha), and $\pi$ is the mathematical constant equal to approximately 3.14 (Kaiser 1983).

As particles are not always horizontal to the ground, the horizontal length of a particle ($l_i$) is converted from the slope length, using

[2.3] $$l_i = \frac{s_i}{\sqrt{1+\frac{p_i^2}{10000}}}$$

where $s_i$ is the field measurement of particle length (m), taken along central axis with a tilt $p_i$ (percent). The number of selected particles at a sample point ($n_k$) was aggregated across the 3 segments

[2.4] $$n_k = \sum_{m=1}^{3} n_{km}$$

From the inclusion probabilities, design-unbiased Horvitz-Thompson (1982) estimators can be derived. The contribution to the aggregate length estimator is the same for each selected particle due to the probability proportional to length design of LIS. Incorporating [2.2], the contribution of each selected particle to the estimated aggregate length of CWD in a stand is:

[2.5] $$\frac{l_i}{\pi_i} = \frac{l_i}{\frac{3L(2l_i)}{10000\pi A}} = 10000\frac{\pi A}{6L}$$

where $l_i$ and $\pi_i$ are previously defined. Summing over the particles selected at a point, an unbiased estimate of aggregate length per hectare is

[2.6] $$\hat{G}_k = \frac{1}{A}\sum_{i=1}^{n_k}\frac{l_i}{\pi_i} = \frac{10000\pi}{2(3L)}\, n_k$$

where $\hat{G}_k$ is the estimated aggregate length (m·ha$^{-1}$) of CWD, at sample point $k$. Note that an estimation of $\hat{G}_k$ does not require individual particle length $l_i$, but rather the number of particles encountered.

### ***2.2.2 Aggregate Volume***

Similar to length estimation, by incorporating the inclusion probabilities, each selected particle contributed

[2.7] $$\frac{v_i}{\pi_i} = 10000 \frac{\pi A}{6L} \frac{v_i}{l_i}$$

units of volume to the estimated stand total, with $v_i$ denoting the volume ($m^3$) of the $i$th particle. As noted by Kaiser (1983) since the point of intersection is determined uniformly at random, individual particle volume can be unbiasedly estimated by

[2.8] $$\hat{v}_i = l_i \frac{\pi}{4} \sum_{j=1}^{q_i} \frac{D_{ij1} D_{ij2}}{10000}$$

where the product of $D_{ij1}$ and $D_{ij2}$, the horizontal and vertical diameters (cm) of the $i$th particle, are summed over $q_i$ lobes. By substituting [2.8] into [2.7] we arrive at

[2.9] $$\frac{\hat{v}_i}{\pi_i} = 10000 \frac{\pi A}{6L} \frac{\hat{v}_i}{l_i} = \frac{\pi^2 A \sum_{j=1}^{q} D_{ij1} D_{ij2}}{24L}.$$

To translate the estimate to volume per hectare, we divide by the stand area. Summing the particle volume by sample point we arrive at the unbiased estimator of aggregate volume

[2.10] $$\hat{V}_k = \frac{1}{A} \sum_{j=1}^{n_k} \frac{\hat{v}_i}{\pi_i} = \frac{\pi^2}{24L} \sum_{\mathrm{i}=1}^{n_k} \sum_{\mathrm{j}=1}^{q} D_{ij1} D_{ij2}$$

where $\hat{V}_k$ is the estimated aggregate volume ($m^3 \cdot ha^{-1}$) at sample point $k$.

### *2.2.3 Abundance*

In a fashion similar to that of length and volume estimation, each particle contributes

[2.11] $$\frac{1}{\pi_i} = 10000 \frac{\pi A}{6L} \frac{1}{l_i}$$

to the estimated particle abundance. Summing this by sample point, gives the unbiased estimator of particle abundance

[2.12] $$\widehat{N}_k = \frac{1}{A} \sum_{i=1}^{n_k} \frac{1}{\pi_i} = \frac{10000\pi}{6L} \sum_{i=1}^{n_k} \frac{1}{l_i}$$

where $\widehat{N}_k$ is the estimated abundance (#·ha$^{-1}$).

These design-based estimators are based on a fixed transect segment length ($L$). Note that to estimate aggregate length ($\widehat{G}_k$), only the particle count needs to be known. Aggregate volume estimates ($\widehat{V}_k$) require particle diameter measurements and abundance estimates ($\widehat{N}_k$) require the length measurements of individual particles. For the development of potential double sampling regression estimators, aggregate length (m·ha$^{-1}$) presents an excellent candidate auxiliary variable, as it is estimated from the simple particle count.

## *2.3 Data Analysis*

### *2.3.1 Univariate Analysis*

The frequency distribution and precision of each attribute was examined on a per stand basis. Frequency histograms were constructed, for visual interpretation of attribute estimate distributions. Following convention, the mean was used as the measure of central tendency, and standard deviation was used to determine the variability among sample point attribute estimates within each stand. For example, standard deviation of the point-level estimates of aggregate length was estimated as

[2.13] $$s_{\widehat{G}} = \sqrt{\frac{\sum_{k=1}^{K} (\widehat{G}_k - \bar{G})^2}{K-1}}$$

where

[2.14] $$\bar{G} = \frac{1}{K}\sum_{k=1}^{K} \hat{G}_k$$

The coefficient of variation (CV), which relates the estimated standard deviation to the estimated mean, was calculated for each attribute *e.g.*,

[2.15] $$CV_{\hat{G}} = \frac{s_{\hat{G}}}{\bar{G}}\ 100\%$$

### ***2.3.2 Multivariate Analysis***

Pairwise combinations of the three stand attribute estimates were plotted and the relationship between attributes was examined. Sample point estimates that deviated markedly from the trend were identified and investigated. The strength of the linear relationship between the attributes of interest in each stand was estimated using Pearson's correlation coefficient ($r_p$). As Pearson's correlation is highly sensitive to extreme data points, a minimum covariance determinant (MCD; Rousseeuw and Leroy 1987) correlation estimator was also used. MCD is a robust covariance estimator that reduces the influence of outlying observations (Fauconnier & Haesbroeck 2009). By using a resampling algorithm, MCD uses a fraction ( > 1/2) of the observations that results in the largest correlation coefficient, thus minimizing the effect of extreme values.

A simple least squares linear regression model was fit to each pairwise attribute combination for each stand. Due to high variability and asymmetry in the distributions, a bootstrap method with 1000 replicates was used to construct 90% confidence intervals for the slope of the regression, standard error of the residual, and the standard deviation of the response variable (i.e. $\hat{V}_k$ or $\hat{N}_k$).

## ***2.4 Analysis of Sampling Times***

As times were recorded for only half of the LIS sample points, a double sampling approach was utilized to estimate mean count time and mean total time. Per segment count time, and per segment total time were regressed against per segment particle count. Here, $t_c$ represents the cost required for phase 1 sampling, during which intersected

particles are only counted; no quantitative (*i.e*. diameter and length) or qualitative (*i.e.* species, decay class) measurements are taken. Phase 2 sampling cost, denoted by $t_t$, represents time required for establishing the transect segment and measuring particle diameters and lengths. The phase 2 sampling effort collected information necessary for calculating both $\hat{V}_k$ and $\hat{N}_k$.

Pearson correlation coefficients were obtained to describe the linear association of count time and total time to particle counts in each stand. A simple linear regression model was also fit to the data for each stand by the least squares method. The variables were not transformed, so the linear models were

[2.17] $$t_{c,km} = a_c n_{km} + b_c + e_{c,km} \quad \text{and}$$
$$t_{t,km} = a_t n_{km} + b_t + e_{t,km}$$

where $t_{\cdot km}$ is the sample time and $n_{km}$ is the number of particles on segment $m$ at sample point $k$, $a_{\cdot}$ is the slope of the regression line, $b_{\cdot}$ is the intercept, and $e_{\cdot km}$ is the unknown error. The slope of the regression was estimated by least squares regression, *e.g.*

[2.18] $$\hat{a}_c = \frac{\sum t_{c,km} n_{km} - \frac{\sum t_{c,km} \sum n_{km}}{M_t}}{\sum n_{km}^2 - \frac{\left(\sum n_{km}\right)^2}{M_t}}$$

where the summations extend over all $M_t$ timed segments in a stand, and other variables are as previously defined. The mean total time and mean count time for all segments in each stand were then estimated with the double sample linear regression estimators

[2.19] $$\hat{t}_c = \bar{t}_c + \hat{a}_c(\bar{n} - \bar{n}_t) \quad \text{and}$$
$$\hat{t}_t = \bar{t}_t + \hat{a}_t(\bar{n} - \bar{n}_t)$$

where $\bar{t}_{\cdot}$ is the average time over the $M_t$ timed segments, $\bar{n}$ is the mean particle count for all segments, and $\bar{n}_t$ is the mean particle count for all timed segments. The variance of these double sampling regression estimators was estimated using, *e.g.*,

[2.20] $$s^2_{\hat{t}_c} = \frac{s^2_{t_c}}{M} + \left(\frac{M-M_t}{M}\right)\frac{s^2_{e_c}}{M_t}$$

where $s^2_{t_c}$ is the sample variance of count times and $s^2_{e_c}$ is the estimated variance of the regression residuals (Thompson 2002). More specifically, the variance of $t_c$ is defined as

[2.21] $$s^2_{t_c} = \frac{\sum_{k=1}^{K}\sum_{m=1}^{3}(t_{c,km} - \bar{t}_c)^2}{M_t - 1}$$

where $\bar{t}_c$ is the mean count time of the $M_t$ timed segments within a stand. The residual variance for the count time against particle count regression ($s^2_{e_c}$) is determined by

[2.22] $$s^2_{e_c} = \frac{\sum_{k=1}^{K}\sum_{m=1}^{3}(t_{c,km} - \hat{b}_c - \hat{a}_c[n_{km}])^2}{M_t - 1}$$

where $\hat{b}_c$ and $\hat{a}_c$ are the estimated intercept and slope of the regression, respectively.

## ***2.5 Double Sampling Optimization & Efficiency***

The optimal ratio of first and second phase sample sizes is a function of both the relative sampling costs and the degree to which the attribute of interest can be predicted from the auxiliary variable. Using results from Thompson (2002) the optimal sample size ratios for estimating $V$ or $N$ from $G$ were estimated for each stand as

[2.23] $$f_V = \sqrt{\frac{s^2_{e,V}}{s^2_{\hat{V}} - s^2_{e,V}} \; \frac{\hat{t}_c}{\hat{t}_t - \hat{t}_c}} \qquad \text{and}$$

$$f_N = \sqrt{\frac{s^2_{e,N}}{s^2_{\hat{N}} - s^2_{e,N}} \; \frac{\hat{t}_c}{\hat{t}_V}}$$

where $f$ is the optimum sample size ratio of phase 2 samples and phase 1 samples, $s^2_{\hat{V}}$ is the variance of $\hat{V}$, $s^2_{\hat{N}}$ is the variance of $\hat{N}$, $s^2_{e,V}$ is the residual variance of $\hat{V}$ against $\hat{G}$

and $s^2_{\hat{e},V}$ is the residual variance of $\widehat{N}$ against $\widehat{G}$, and all other variables are as previously defined.

The efficiency of double sampling relative to traditional LIS also can be expressed in terms of the error and costs associated with the attribute estimators. We used a comparison of the variance ratios to the cost ratios,

[2.24]
$$\frac{\hat{t}_t - 2\hat{t}_c}{\hat{t}_t} \geq \frac{s^2_{\hat{e},V}}{s^2_V} \quad \text{and}$$

$$\frac{\hat{t}_t - 2\hat{t}_c}{\hat{t}_t} \geq \frac{s^2_{\hat{e},N}}{s^2_N}$$

where the variance ratio is right of the inequality, and the cost ratio is to the left to determine relative efficiency. The variance ratios were estimated using 90% bootstrap confidence intervals. If the cost ratio is indeed greater than or equal to the variance ratio, there is an increase in efficiency associated with double sampling.

# 3. RESULTS AND DISCUSSION

## *3.1 Stands*

Stands were given identifiers derived from the common names of the most abundant species relative to basal area (Table 3.1). Two stands were co-dominated by Douglas-fir and western larch, denoted DL1 and DL2. Two stands were dominated by ponderosa pine and denoted PP1 and PP2. Two stands dominated by Douglas-fir were labeled DF1 and DF2, and the stand dominated by lodgepole pine was labeled LP1.

**Table 3.1** Stand estimates of species relative abundance, age, elevation, aspect, basal area (BA) and mean travel time. Species relative abundance was based on basal area.

| | Relative Abundance (%) | | | | | Stand | Stand Average | | | |
|---|---|---|---|---|---|---|---|---|---|---|
| ID | PP | DF | WL | LP | ES | Age (yrs) | Elevation (m) | Aspect | BA ($m^2 \cdot ha^{-1}$) | Travel time ($m \cdot min^{-1}$) |
| DL1 | 3 | 42 | 55 | - | - | > 150 | 1283 | N | 44.76 | 15.46 |
| DL2 | 3 | 53 | 44 | - | - | 80-100 | 1168 | N | 32.47 | 19.10 |
| PP1 | 68 | 32 | - | - | - | 90-110 | 1306 | SE | 15.86 | 14.36 |
| PP2 | 63 | 37 | - | - | - | 90-110 | 1458 | S | 27.26 | 17.99 |
| DF1 | - | 60 | 21 | 19 | - | 50-70 | 1306 | NW | 20.66 | 12.13 |
| DF2 | - | 70 | 18 | 10 | 2 | 80-100 | 1505 | NW | 30.30 | 26.03 |
| LP1 | - | - | - | 100 | - | 70-90 | 1859 | NW | 22.67 | 8.86 |

Basal area of the selected stands ranged from approximately 16 $m^2 \cdot ha^{-1}$ in PP1 to 45 $m^2 \cdot ha^{-1}$ in DL1. Stands with similar dominant species were unique in estimated stand basal area. For example, the estimated basal area in PP1 was approximately half that of PP2.

The average travel time ranged from approximately 8.86 to 26.03 meters per minute in LP1 and DF2, respectively. There was no obvious relationship between estimated stand basal area or slope and mean travel time. In fact, it should be noted that the stand with the largest estimate of basal area had only a moderate estimate of mean travel time. Similarly, the stand with the largest travel time estimate had a moderate basal area estimate, relative to the other stands.

Interestingly, the mean travel time for a stand appeared to be inversely related to mean particle abundance (Fig. 3.1). Although our data is too limited to make inference on such a relationship, it would seem reasonable that mobility is more difficult, such that travel would be slower in stands with more CWD.

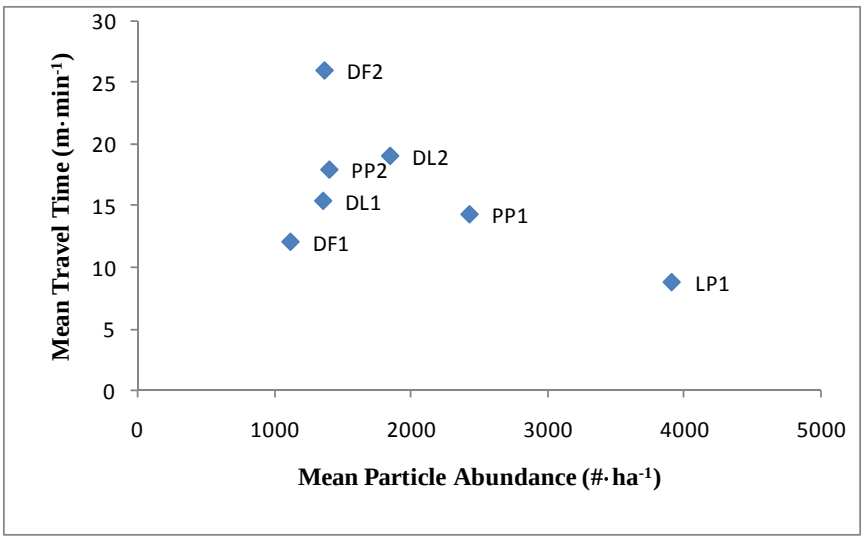


**Figure 3.1** Estimated travel time for selected stands as related to particle abundance.

## *3.2 CWD Attributes*

### *3.2.1 Univariate Analysis*

Following [2.2] through [2.12], estimates of aggregate length, aggregate volume and abundance were calculated for individual sampling points for each of the 7 selected stands (Table 3.2). Variability of the estimators is given by the standard deviation [2.13], and coefficient of variation [2.14].

Stand-level estimates of aggregate length ranged from a low of 3152 m· ha$^{-1}$ in PP2 to a high of 27053 m· ha$^{-1}$ in LP1. Stand LP1 also had the lowest CVs relative to the other stands, estimated at 27%. LP1 was an approximately even-aged stand, and lodgepole pine was the only species encountered in basal area samples. Recalling that $\hat{G}_k$ is based on the simple particle count, the low CV suggests CWD distribution was rather homogenous among LP1 sample points, when compared to the other stands. The largest variability was found in stand DF1, which had a relatively low mean of 3374 m· ha$^{-1}$. This could be a result of spatial heterogenity of particles, and possibly a clumped or patchy distribution.

Mean aggregate volume ranged from 41 m$^3$· ha$^{-1}$ in DL1, to 209 m$^3$· ha$^{-1}$ in stand LP1. Again, LP1 had a relatively low CV of approximately 50%. $\hat{V}_k$ is determined from diameter measurements, meaning a low CV results from encountering similar numbers of particles with a narrow range of diameters. The diameter measurements in LP1 ranged

from approximately 1 to 37 cm. Conversely, the high CV of stand DF1 can be attributed to a large range of diameters, measuring from less than 1 to 147 cm.

**Table 3.2** Stand attribute estimates, standard devation and coefficient of variation (%) of CWD attribute estimates.

| ID | mean | *s* | *CV* |
|---|---|---|---|
| *Aggregate Length ($m \cdot ha^{-1}$)* | | | |
| DL1 | 4413 | 2002 | 45.36 |
| DL2 | 4760 | 2900 | 60.92 |
| PP1 | 4885 | 3057 | 62.57 |
| PP2 | 3152 | 1549 | 49.14 |
| DF1 | 3374 | 2828 | 83.80 |
| DF2 | 4025 | 1881 | 46.72 |
| LP1 | 27053 | 7321 | 27.06 |
| *Aggregate Volume ($m^3 \cdot ha^{-1}$)* | | | |
| DL1 | 41 | 36 | 88.30 |
| DL2 | 55 | 50 | 91.77 |
| PP1 | 42 | 35 | 82.78 |
| PP2 | 55 | 27 | 49.88 |
| DF1 | 48 | 64 | 134.39 |
| DF2 | 45 | 43 | 95.78 |
| LP1 | 209 | 105 | 50.24 |
| *Abundance ($\# \cdot ha^{-1}$)* | | | |
| DL1 | 1356 | 1069 | 78.84 |
| DL2 | 1847 | 2004 | 108.47 |
| PP1 | 2430 | 1881 | 77.41 |
| PP2 | 1401 | 797 | 56.88 |
| DF1 | 1115 | 930 | 83.41 |
| DF2 | 1366 | 823 | 60.25 |
| LP1 | 3914 | 2340 | 59.78 |

Mean $\widehat{N}_k$ ranged from 1115 particles per hectare in DF1 to 3914 particles per hectare in LP1. Recalling that $\widehat{N}_k$ is determined from particle lengths, the variability in $\widehat{N}_k$ results in part from the variability in particle lengths. Stands PP2 and LP1 had the lowest CVs of the selected stands, suggesting low variability among point estimates of abundance in these stands. In contrast, DL2 had the largest CV of the stands, which implies high variability among sample points. Considering the co-dominance of western larch and Douglas-fir, as well as the presence of ponderosa pine (Table 3.1), this is not

surprising. As any carpenter well knows, wood density varies with species. As trees die and fall, the wood density and morphology influence the probability of stem breakage (Baker *et al*. 2004; Cornwell *et al*. 2009). Western larch, Douglas-fir and ponderosa pine will therefore differ in resistance to stem breakage, resulting in various lengths of CWD among species.

Although differences in forest type may be a main cause for variability in CWD estimates, sample design, specifically transect length, has been shown to affect estimator variability. For example, Woldendorp and others (2004) found that at all study locations, the CV decreased as the number of intersected particles increased for a given length of transect. That is, longer transects encountered more particles than shorter transects, resulting in more precise estimates of CWD attributes.

Variability of aggregate volume and abundance estimates in the present study are similar to those reported for Australia (Woldendorp *et al*. 2004). In a comparison study of LIS transect lengths, the authors reported CVs for volume estimates ranging from 57-363% (Woldendorp *et al*. 2004). In a similar study in British Columbia, Nemec and Davis (2002) reported CVs for aggregate volume of approximately 13-66%, and CVs of abundance ranging from 27-75%. Interestingly, a sub category of particles with a large end diameter greater than 60 cm was analyzed separately. The variability in this category was quite extreme relative to the all-inclusive CWD category, with CVs ranging from 22-179% for aggregate volume and 38-150% for abundance (Nemec and Davis 2002). The high variability in estimates of large CWD suggests precision could be increased if attributes were estimates separately for extreme size classes.

### ***3.2.2 Multivariate Analysis***

The distribution of sample point attribute estimates is illustrated with a frequency histogram for each stand, in Figures 3.2- 3.8. The relationship of $\hat{V}_k$ and $\hat{N}_k$ relative to $\hat{G}_k$ is also shown for each of the 7 stands in the lower panel of the figures. A locally weighted scatterplot smoothing (LOWESS) model, which minimizes the effect of outlying points and a least squares regression line were fit to the data. Similarly, the relationship of $t_{tm}$ and $t_{cm}$, to $n_{kj}$ are shown in part f of Figures 3.2 - 3.8, with least squares regression models fit to each.

Interestingly, only the lodgepole pine stand (LP1), and both stands co-dominated by Douglas-fir and western larch (DL1 and DL2) produced relatively uniform distributions of $\hat{G}_k$ , whereas the distribution is right skewed in the remaining 4 stands. In all 7 stands, the distribution of both $\hat{V}_k$ and $\hat{N}_k$ are right skewed. This skewness results from extreme values of the attribute estimates. In this case, the extreme values are much larger than the other point estimates in the stand. As mentioned previously, PP2 and LP1 had the lowest $CV_{\hat{N}}$ of the stands, whereas DF2 had the highest. This variability is reflected in the frequency distribution figures. While all stands exhibit right skewed abundance distributions, the most extreme case is DL2, whereas PP2 and LP1 were the least severe.

The extreme sample point estimates are also highlighted in Figures 3.2-3.8 e and f. The extreme values of $\hat{V}_k$ and $\hat{N}_k$ are colored green and orange respectively. The regression of $\hat{V}_k$ against $\hat{G}_k$ has extreme sample points with both high influence and leverage on the least squares regression line. Recalling that volume is estimated using diameter measurements, these large volume estimates are a consequence of encountering either many particles or particles with extremely large diameters, relative to other particles. For example, although the mean diameter of selected particles in DL1 was approximately 8.1 cm, the maximum diameter measured was 70 cm. Although the $\hat{V}_k$ of this sample point was extremely high, there are 3 other points in the stand with even higher estimates. It should therefore be noted that variability and skewness in estimates can definitely result from sampling error, as opposed to measurement error in the present study.

In the same way, the largest and smallest $\hat{N}_k$ values in Figures 3.2-3.8 result from abnormally short particles and long particles at those sample points. Considering that with the exception of PP2, all stands encountered between 0-14 particles per segment (Fig 3.2-3.8 graph f), each particle can have a considerable effect on the sample point estimate. This is especially true when fewer particles were encountered. Although individual estimates are used to develop the relationship between attributes, predictions allowed by regression double sampling are generally aimed at mean estimates, rather than individual point estimates. Fortunately, mean estimates are more accurate than individual estimates (Ott & Longnecker 2001).

The least squares regression line serves as an estimation tool in double sampling estimates. As shown in [2.19], the regression relationship serves to adjust the simple estimate based only on the second phase sample in accordance with how the second and first phase samples differ.

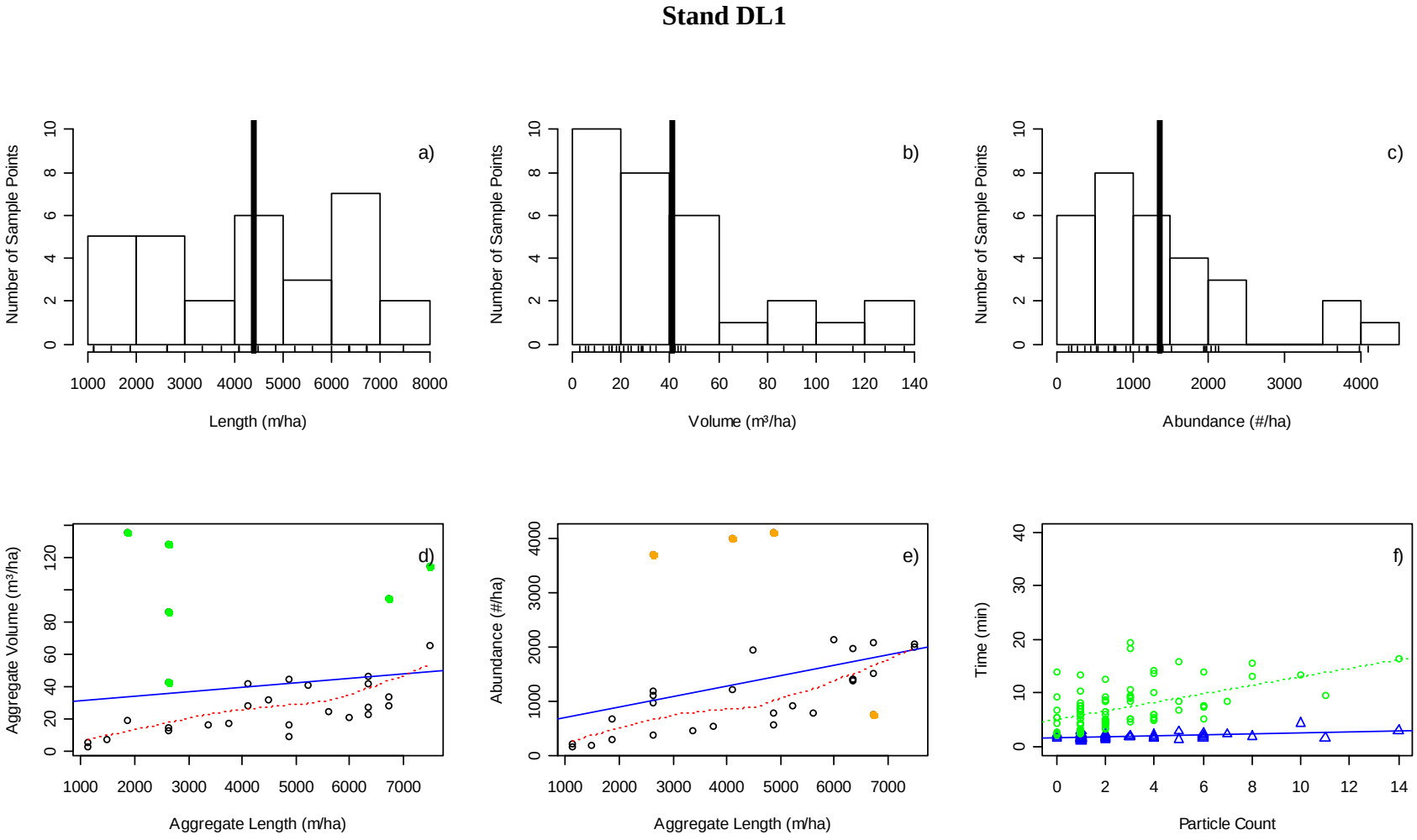


**Figure 3.2** Stand DL1 frequency distributions of $\hat{G}_k$, $\hat{V}_k$ and $\hat{N}_k$ (graphs a, b, and c, respectively), where the mean is indicated by the bold vertical line. Graphs d and e show the relationship between point estimates of attributes, with outliers marked with solid colored green and orange circles, respectively; the solid blue line indicates the linear least squares regression, and the dashed red line indicates the LOESS fit. Graph f shows segment particle count as it affects count time (blue triangles) and total time (green circles).

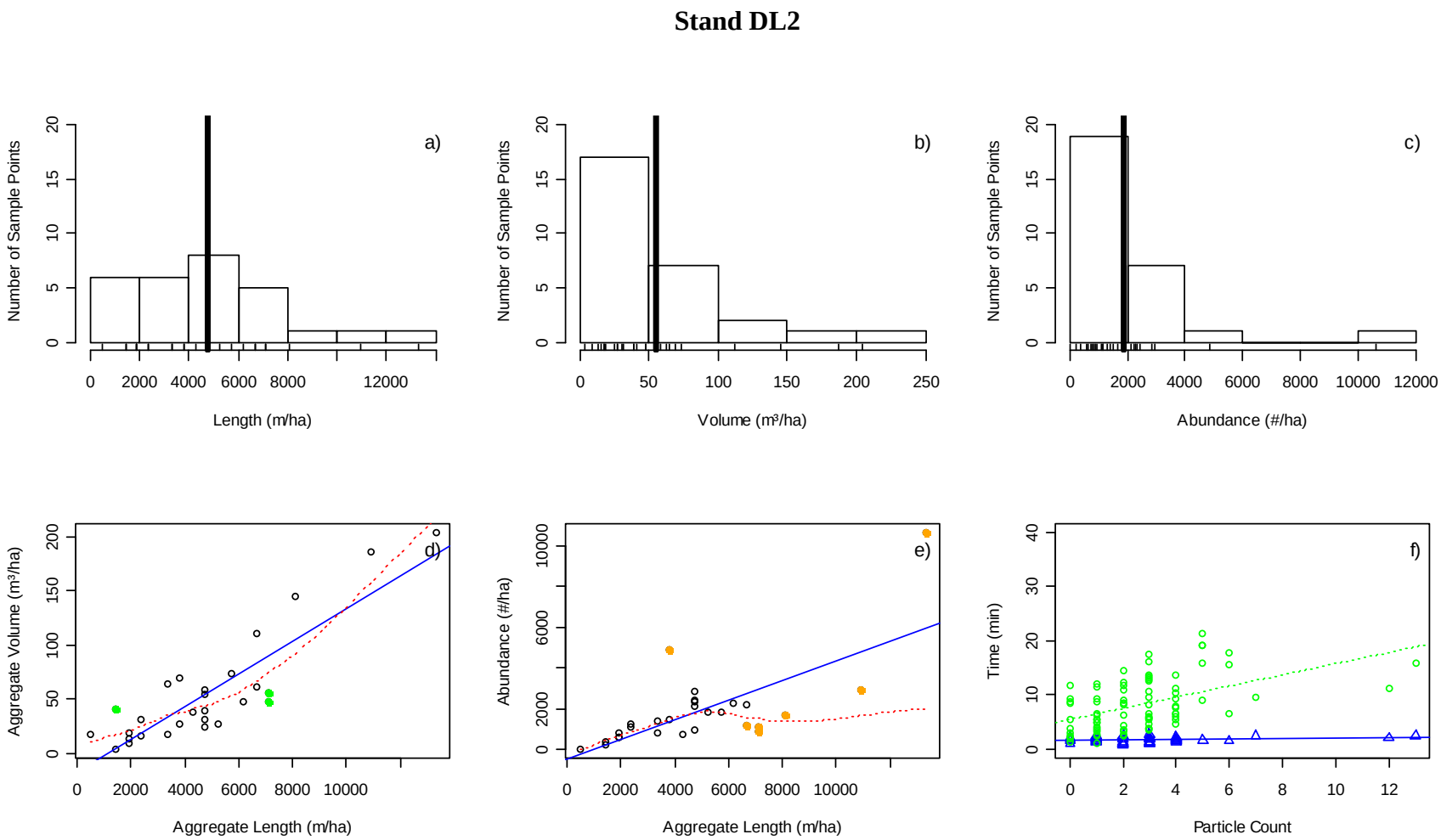


**Figure 3.3** Summary of CWD sampling results for Stand DL2 (see Fig. 3.2 for description).

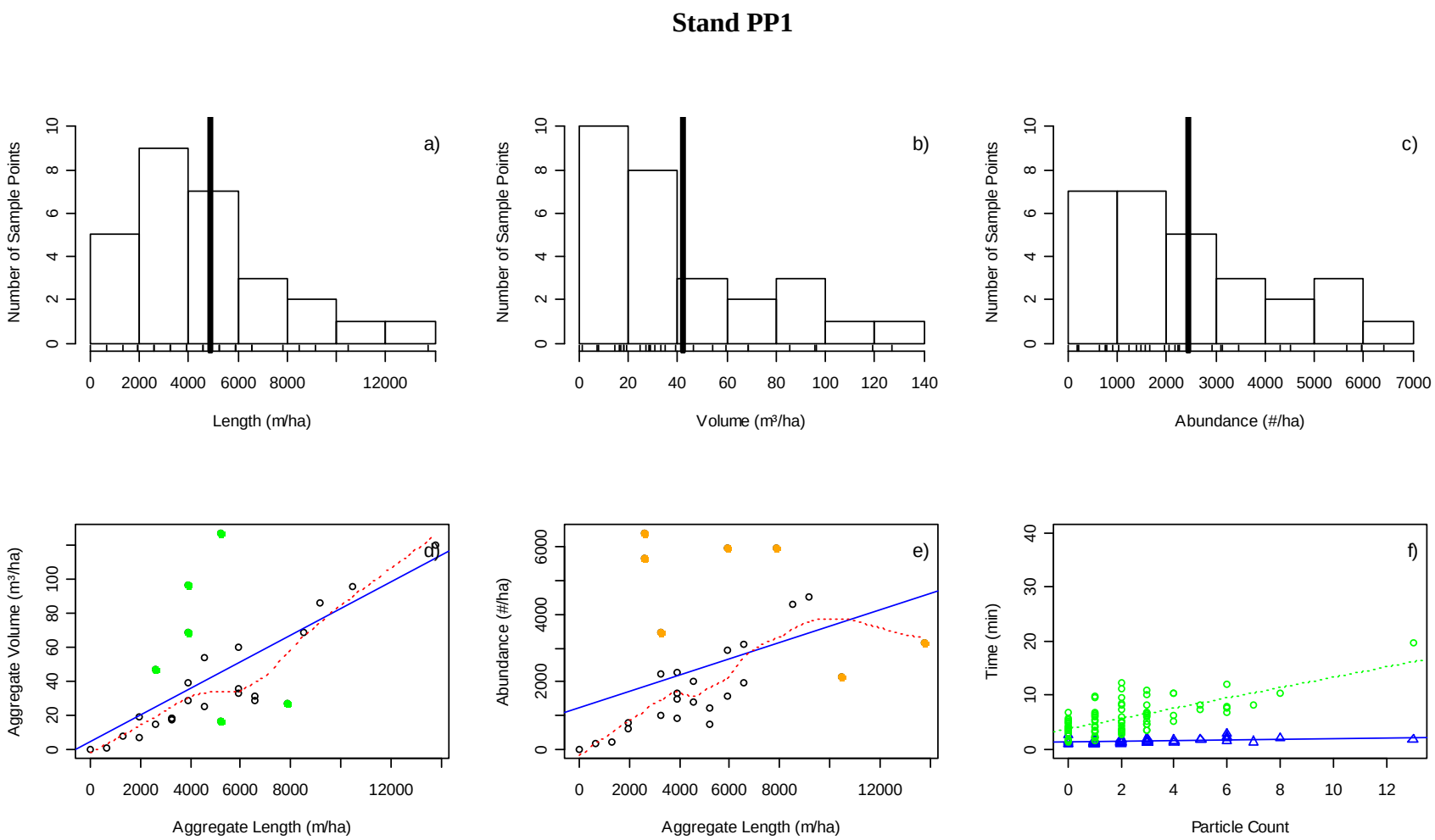


**Figure 3.4** Summary of CWD sampling results for Stand PP1 (see Fig. 3.2 for description).

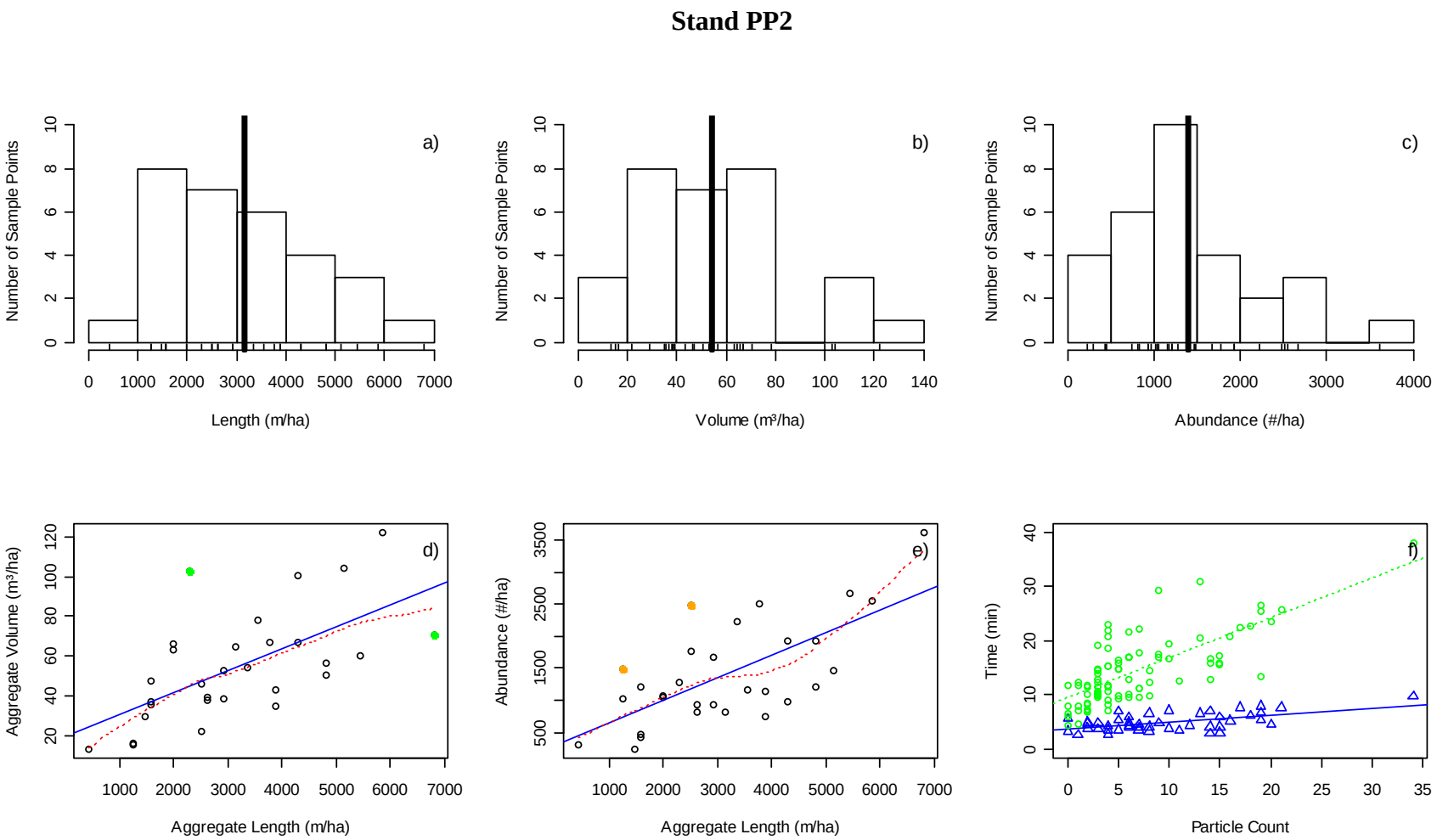


**Figure 3.5** Summary of CWD sampling results for Stand PP2 (see Fig. 3.2 for description).

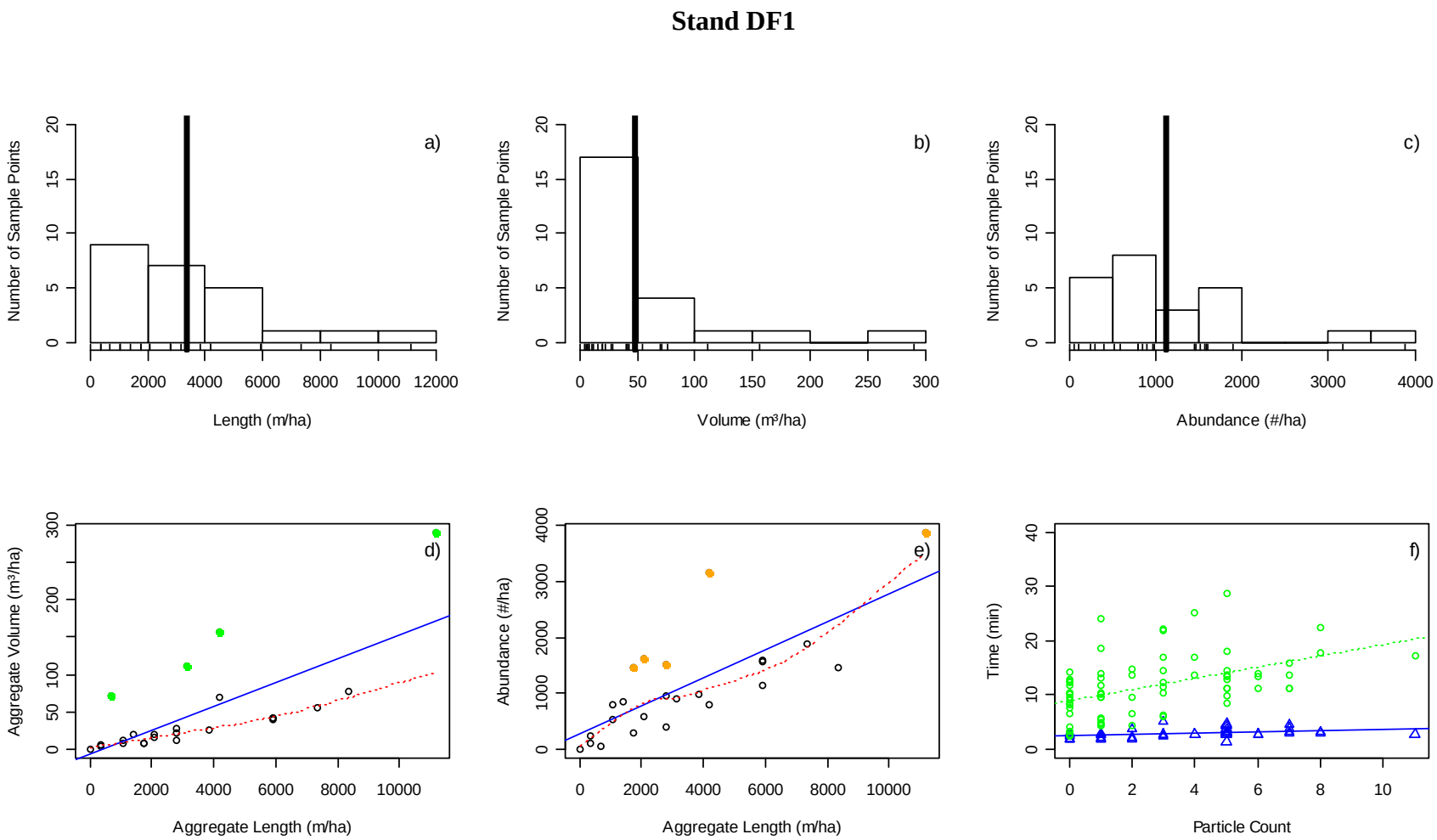


**Figure 3.6** Summary of CWD sampling results for Stand DF1 (see Fig. 3.2 for description).

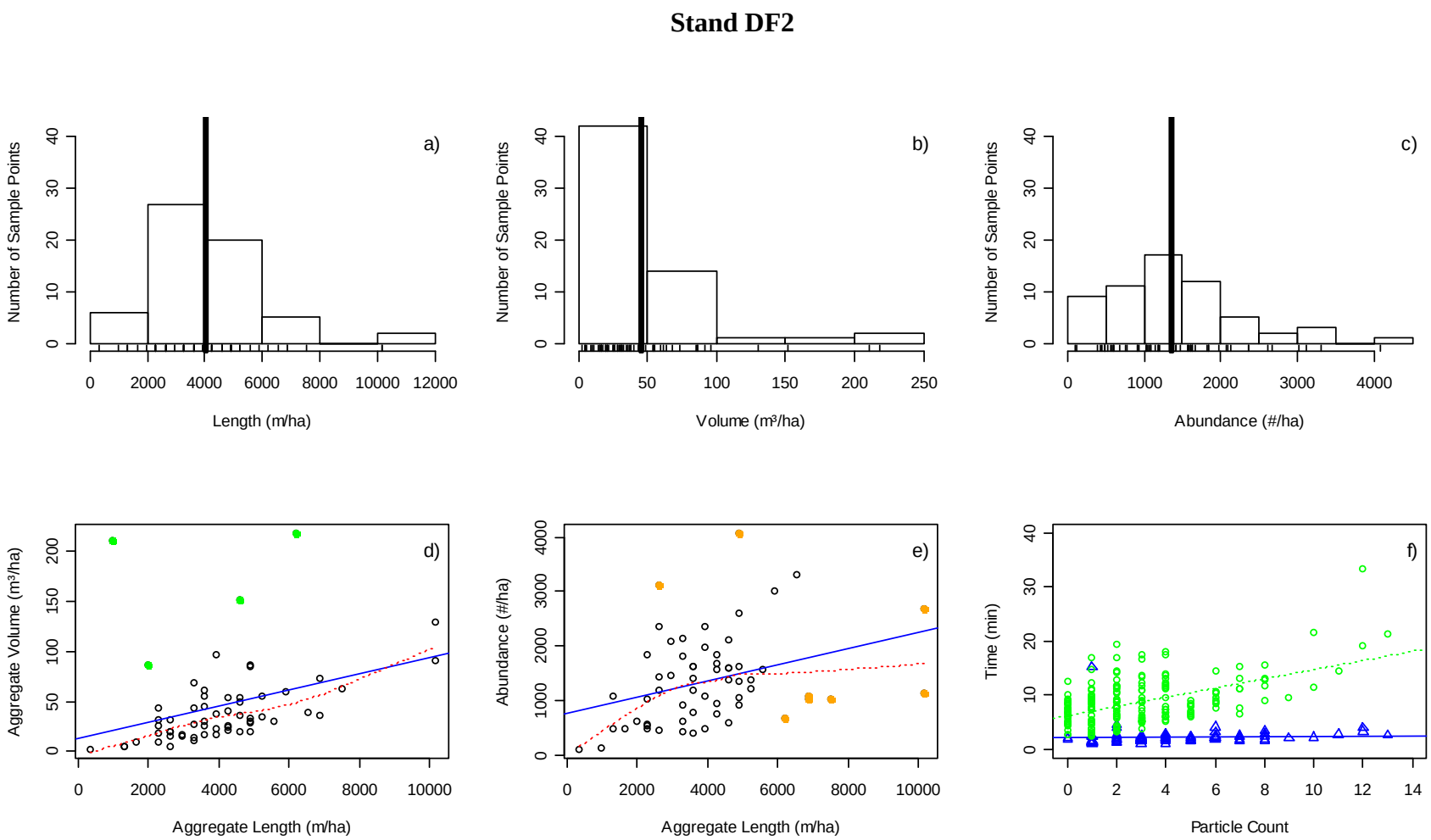


**Figure 3.7** Summary of CWD sampling results for Stand DF2 (see Fig. 3.2 for description).

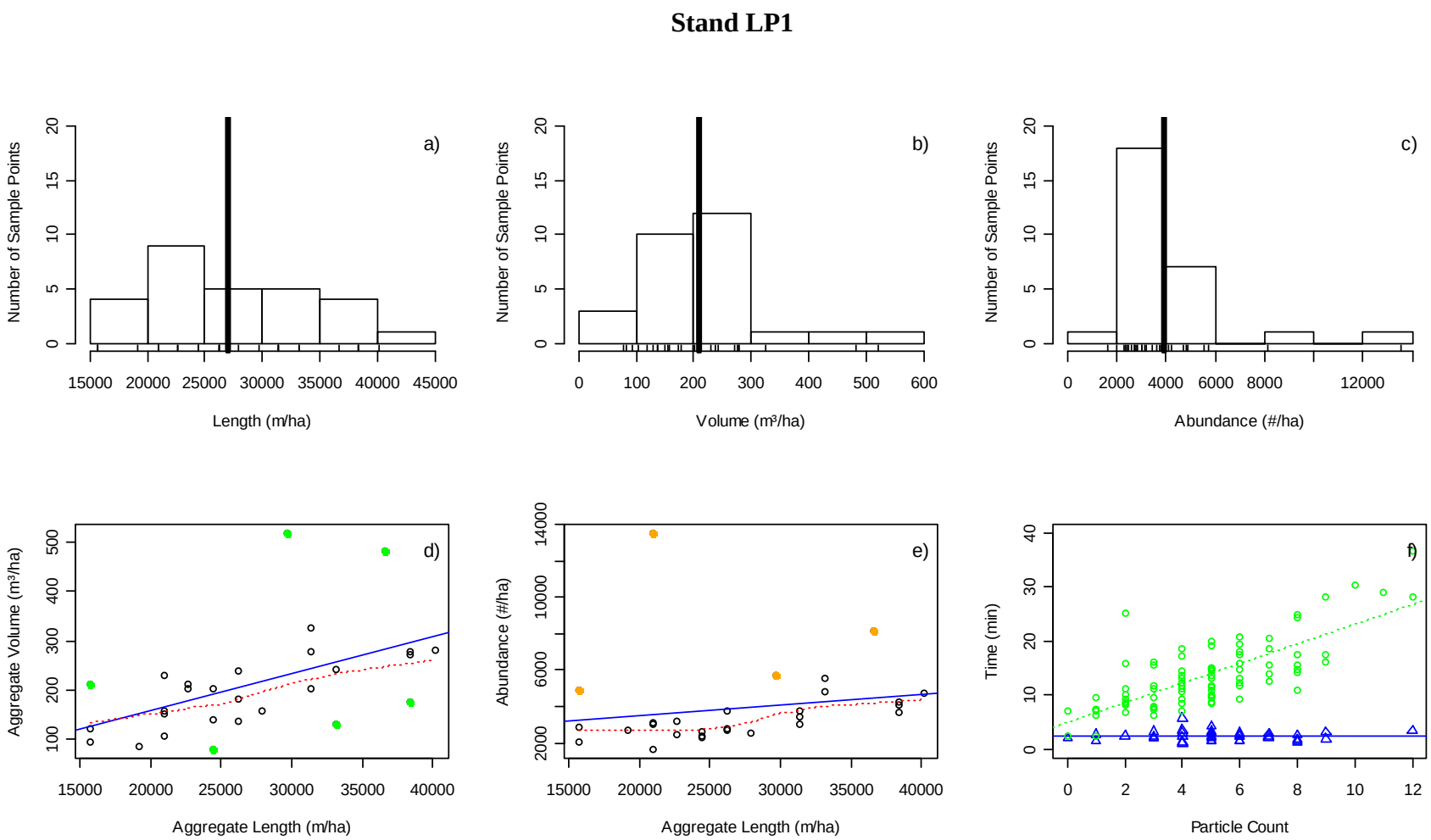


**Figure 3.8** Summary of CWD sampling results for Stand LP1 (see Fig. 3.2 for description).

The two correlation coefficient estimators, Pearson and MCD, produced substantially different correlation coefficients for $\hat{G}_k$ to both $\hat{V}_k$ and $\hat{N}_k$ (Table 3.3). The MCD method was clearly more resistant to outlying data points, and for the most part gave larger estimates of attribute correlation. In the few cases in which the MCD method produced a lower correlation coefficient than Pearson, the outliers removed from consideration were likely extreme estimates of aggregate length, rather than aggregate volume or abundance. The MCD correlation was preferred for the present study and coefficients were used in subsequent comparisons, rather than Pearson's.

**Table 3.3** Estimates of Pearson and MCD correlation coefficients for sample point estimates of aggregate volume to aggregate length, and abundance to aggregate length. Stands with a MCD correlation coefficient less than the Pearson correlation coefficient are in bold.

| | **Volume: Length** | | **Abundance : Length** | |
|---|---|---|---|---|
| *ID* | *Pearson* | *MCD* | *Pearson* | *MCD* |
| DL1 | 0.1490 | 0.6726 | 0.3589 | 0.7849 |
| DL2 | **0.8729** | **0.8279** | 0.6945 | 0.8267 |
| PP1 | 0.6833 | 0.8004 | 0.3932 | 0.7507 |
| PP2 | 0.6282 | 0.7312 | **0.685** | **0.5077** |
| DF1 | 0.7068 | 0.9430 | **0.7665** | **0.6806** |
| DF2 | 0.3491 | 0.7195 | **0.3384** | **0.3181** |
| LP1 | 0.5298 | 0.5986 | 0.1879 | 0.7199 |

The MCD correlation coefficients of $\hat{V}_k$ to $\hat{G}_k$ ranged from 0.59 for LP1, to 0.94 for DF1. For the correlation of $\hat{N}_k$ to $\hat{G}_k$, MCD correlation coefficients ranged from 0.32 to 0.83 among the 7 stands. In all but two stands, DL1 and LP1, the correlation of $\hat{V}_k$ to $\hat{G}_k$ is stronger than the correlation of $\hat{N}_k$ to $\hat{G}_k$.

## ***3.3 Sampling Times***

In order to assess the efficiency of double sampling for $V$ and $N$, linear regression estimates of mean phase 1 (Table 3.4) and phase 2 (Table 3.5) sample times were obtained. Count time (phase 1 sample time) and total time (phase 2 sample time) are both positively correlated to particle count. Although the count time to particle count correlation is quite weak, the variance of double sampling estimates for both count time and total time are less than those of traditional estimates. This demonstrates the benefits

of double sampling, even in cases when the correlation coefficient is low. Due to the precision gained, double sample linear regression estimates of mean sample time were used for determining optimal sample sizes and efficiency of LIS double sampling methods.

**Table 3.4** Estimated mean count time for each stand, with simple random sampling estimates on the left based only on timed segments, and estimates on the right representing double sampling linear regression estimates (Eq. 2.18-2.20).

| | Simple Random Sampling | | | | | | Double Sampling | | | |
|---|---|---|---|---|---|---|---|---|---|---|
| ID | $M_t$ | $\bar{n}_t$ | $\bar{t}_c$(min) | $s_{t_c}$(min) | $\hat{a}_c$ (min) | $r^2_{MCD}$ | M | $\bar{n}$ | $\hat{t}_c$ (min) | $s_{t_c}$(min$^2$) |
| DL1 | 45 | 3.244 | 1.964 | 0.761 | 0.08 | 0.206 | 90 | 2.633 | 1.912 | 0.097 |
| DL2 | 42 | 2.902 | 1.798 | 0.690 | 0.04 | 0.230 | 84 | 2.655 | 1.788 | 0.091 |
| PP1 | 42 | 2.925 | 1.585 | 0.647 | 0.06 | 0.040 | 84 | 2.071 | 1.530 | 0.082 |
| PP2 | 45 | 9.818 | 4.994 | 1.271 | 0.13 | 0.125 | 90 | 6.778 | 4.590 | 0.194 |
| DF1 | 36 | 3.667 | 2.872 | 0.932 | 0.13 | 0.701 | 72 | 2.597 | 2.737 | 0.145 |
| DF2 | 90 | 4.292 | 2.253 | 1.236 | 0.03 | 0.224 | 180 | 3.011 | 2.218 | 0.147 |
| LP1 | 42 | 5.220 | 2.489 | 0.942 | 0.01 | 0.224 | 84 | 4.821 | 2.486 | 0.142 |

**Table 3.5** Estimated mean total time for each stand, with simple random sampling estimates on the left based only on timed segments, and estimates on the right representing double sampling linear regression estimates (Eq. 2.18-2.20).

| | Simple Random Sampling | | | | | | Double Sampling | | | |
|---|---|---|---|---|---|---|---|---|---|---|
| ID | $M_t$ | $\bar{n}_t$ | $\bar{t}_t$(min) | $s_{t_t}$(min) | $\hat{a}_t$ (min) | $r^2_{MCD}$ | M | $\bar{n}$ | $\hat{t}_t$(min) | $s_{t_t}$ (min$^2$) |
| DL1 | 45 | 3.244 | 5.285 | 1.747 | 0.94 | 0.860 | 90 | 2.633 | 4.711 | 0.215 |
| DL2 | 42 | 2.902 | 5.205 | 1.691 | 0.90 | 0.853 | 84 | 2.655 | 4.982 | 0.241 |
| PP1 | 42 | 2.925 | 5.045 | 1.857 | 1.23 | 0.723 | 84 | 2.071 | 3.999 | 0.240 |
| PP2 | 45 | 9.818 | 14.593 | 2.618 | 0.87 | 0.724 | 90 | 6.778 | 11.959 | 0.421 |
| DF1 | 36 | 3.667 | 9.421 | 2.291 | 1.61 | 0.915 | 72 | 2.597 | 7.704 | 0.396 |
| DF2 | 90 | 4.292 | 7.897 | 2.167 | 1.32 | 0.850 | 180 | 3.011 | 6.211 | 0.274 |
| LP1 | 42 | 5.220 | 11.635 | 2.147 | 1.70 | 0.257 | 84 | 4.821 | 10.957 | 0.344 |

## ***3.4 Double Sampling Optimization & Efficiency***

Incorporating the estimates of residual error of the linear regression of $\hat{V}_k$ on $\hat{G}_k$ and $\hat{N}_k$ on $\hat{G}_k$, optimal sample sizes for regression double sampling were calculated (Table 3.6 and 3.7; [ 2.21]).

**Table 3.6** Phase 2 to phase 1 optimal sample size ratios for volume estimations.

| Aggregate Volume | | | | |
|---|---|---|---|---|
| ID | $s_{\hat{V}}$ | $s_{e,V}$ | $\hat{t}_c/\hat{t}_t$ | $f_V$ |
| DL1 | 36.14 | 36.37 | 0.41 | 1.00 |
| DL2 | 50.23 | 25.02 | 0.36 | 0.34 |
| PP1 | 35.17 | 26.17 | 0.38 | 0.69 |
| PP2 | 27.21 | 21.54 | 0.38 | 0.80 |
| DF1 | 63.95 | 46.25 | 0.36 | 0.62 |
| DF2 | 43.50 | 41.11 | 0.36 | 1.00 |
| LP1 | 105.22 | 90.94 | 0.23 | 0.82 |

Based on the least squares linear regression of $\hat{V}_k$ against $\hat{G}_k$, and the estimated costs of phase 1 and phase 2 sampling, the optimum number of phase 2 samples should be approximately 34-100% of the phase 1 sample size. By definition, double sampling requires that the phase 2 sample size be less than the phase 1 sample size. For aggregate volume estimation, the high residual error requires some phase 2 sample sizes be larger than phase 1, thus negating double sampling in these stands. Furthermore, the variance of $\hat{V}_k$ for stand DL1 is less than the residual variance, signifying that $\hat{G}_k$ does not account for any of the variability in $\hat{V}_k$ and that double sampling is not beneficial in this stand.

**Table 3.7** Phase 2 to phase 1 sample size ratios for abundance estimations.

| Abundance | | | | |
|---|---|---|---|---|
| ID | $s_{\hat{N}}$ | $s_{e,N}$ | $\hat{t}_c/\hat{t}_t$ | $f_N$ |
| DL1 | 1069.00 | 1015.45 | 0.41 | 1.00 |
| DL2 | 2003.70 | 1469.07 | 0.36 | 0.65 |
| PP1 | 1880.77 | 1762.23 | 0.38 | 1.00 |
| PP2 | 797.03 | 590.96 | 0.38 | 0.68 |
| DF1 | 930.40 | 610.934 | 0.36 | 0.52 |
| DF2 | 823.14 | 781.238 | 0.36 | 1.00 |
| LP1 | 2339.60 | 2341.712 | 0.23 | 1.00 |

The optimum number of phase 2 samples, based the least squares linear regression of $\hat{N}_k$ against $\hat{G}_k$ and the estimated costs of phase 1 and phase 2 sampling, is 52-100% of the phase 1 sample size. The optimal phase 2 sample sizes for stands DL1, PP1, DF2 and LP1 are equal to the phase 1 sample sizes, indicating that double sampling is not beneficial. Moreover, the residual standard error for stand LP1 is greater than the

variance of $\widehat{N}_k$, suggesting that double sampling is not advantageous for this attribute with this auxiliary variable in this stand.

Optimum sample sizes for both $V$ and $N$ double sampling schemes are highly variable. Much of this variability can be attributed to the high residual error of the regression model and the underlying $\widehat{V}_k$ and $\widehat{N}_k$. Stands with high residual error relative to the variance of the point estimates require large sample size ratios. Conversely, stands with low residual error relative to the variance of the point estimates call for low optimal sample size ratios.

Following [2.22], we investigated the difference in sampling costs (*i.e.* time) relative to the standard deviation of the variable of interest (*i.e.* $\widehat{V}_k$ or $\widehat{N}_k$), and the residual standard error of the regression (Table 3.8 and 3.9). If the cost ratio is greater than the variance ratio, efficiency can be increased through double sampling. If the cost ratio falls within the upper and lower bounds of a 90% confidence intervals for the variance ratio, the efficiency of double sampling is questionable.

**Table 3.8** Efficiency of double sampling for aggregate volume estimation.

| Aggregate Volume | | | | |
|---|---|---|---|---|
| Stand | Variance Ratio | | Cost | Efficiency |
| ID | Lower | Upper | Ratio | gains |
| DL1 | 0.920 | 1.018 | 0.188 | no |
| DL2 | 0.342 | 0.708 | 0.282 | no |
| PP1 | 0.504 | 0.921 | 0.235 | no |
| PP2 | 0.628 | 0.946 | 0.232 | no |
| DF1 | 0.490 | 0.934 | 0.289 | no |
| DF2 | 0.744 | 0.966 | 0.286 | no |
| LP1 | 0.746 | 0.967 | 0.546 | no |

In all 7 selected stands, the cost ratio was below the confidence intervals for the variance ratio, signifying that double sampling for volume estimation is not warranted. Similarly, the cost ratio of the 7 stands is less than the lower bound of the variance ratio confidence interval, thus the present double sampling scheme is not beneficial for abundance estimation.

**Table 3.9** Efficiency of double sampling for abundance estimation.

| Abundance | | | | |
|---|---|---|---|---|
| Stand ID | Variance Ratio | | Cost Ratio | Efficiency gains |
| | Lower | Upper | | |
| DL1 | 0.822 | 1.016 | 0.188 | no |
| DL2 | 0.545 | 0.987 | 0.282 | no |
| PP1 | 0.805 | 1.017 | 0.235 | no |
| PP2 | 0.564 | 0.918 | 0.232 | no |
| DF1 | 0.429 | 0.857 | 0.289 | no |
| DF2 | 0.807 | 1.019 | 0.286 | no |
| LP1 | 0.806 | 1.019 | 0.546 | no |

## ***3.5 General Discussion***

Although double sampling has allowed for precision gains or cost savings in many cases (*e.g*. Dellenbaugh *et al*. 2007; Fule & Covington 1994), the use of aggregate length as an auxiliary variable for estimation of CWD aggregate volume or abundance following the LIS strategy is not advantageous in these stands. With double sampling, the auxiliary variable and variable of interest must be well and positively correlated for gains to be made. In the present study, the variables were indeed positively correlated, but the strength of the relationship was rather weak and difficult to assess due to high variability in attribute estimates within a stand. The weak correlation is reflected in the large residual error of the regression, thus decreasing precision of the double sampling linear regression estimator, relative to standard single phase LIS estimators. Similar to our use of the robust correlation measure MCD, regression models that are resistant to outlying data points may provide a more precise method of regression estimation following double sampling. Further studies of robust regression techniques could warrant the application of double sampling to LIS, using the variables investigated in the present study.

Another contributing factor to the lack of double sampling benefit found in this study is the cost ratio of phase 2 to phase 1 sampling efforts. As shown in Figure 1.1, the greater the difference in sampling cost between the two phases, the lower the correlation threshold needed for double sampling benefits to accrue. Shiver and Borders (1996) give

examples ranging from 1:5 to 1:100 for phase 1 to phase 2 sampling costs (Table 3.10). It should be noted that these sample sizes are the same for both independent and dependent phase 2 samples, so long as the sample size is reasonably large (Shiver & Borders 1996). As illustrated in Tables 3.6 and 3.7, phase 1 sampling cost was approximately 23-41% of phase 2 sampling costs. This equates to a ratio of phase 1 to phase 2 costs ranging from approximately 1:2 to 1:4 for the selected stands. This cost difference is considerably less than needed for efficient application of double samplingand requires a very strong correlation of the response and explanatory variables.

**Table 3.10** Optimal percentage of phase 1 samples to include as phase 2 samples, assuming simple random sampling is used in both phases (from Shiver & Borders 1996).

| Relative Cost | Correlation with auxiliary variable | | | | | |
|---|---|---|---|---|---|---|
| Phase 1: Phase 2 | 0.5 | 0.6 | 0.7 | 0.8 | 0.9 | 0.95 |
| 1:05 | 77 | 60 | 46 | 36 | 22 | 15 |
| 1:10 | 55 | 42 | 32 | 24 | 15 | 10 |
| 1:15 | 45 | 34 | 26 | 19 | 13 | 8 |
| 1:20 | 39 | 30 | 23 | 17 | 11 | 7 |
| 1:30 | 32 | 21 | 19 | 14 | 9 | 6 |
| 1:50 | 24 | 19 | 14 | 11 | 7 | 5 |

Additionally, phase 2 sampling efforts included measurements necessary for estimation of both aggregate volume and abundance. In this case, aggregate length was used for estimation of two attributes, rather than one, requiring measurement of particle diameter and length. Greater cost differences would likely be observed had only one attribute been estimated, and therefore only diameter or only length would be measured in the second phase. From practical experience, we can speculate that the length measurements are more time intensive than intersect diameter measurements, as they require traveling away from the transect. In stands with a large quantity of CWD, travel can be very difficult and time consuming.

Furthermore, imprecise sample cost estimates could confound the ability to confidently assess the efficiency of double sampling. The use of regression double sampling to estimate costs in the present study provides an example of precision gains relative to traditional sampling. In fact, even with a weak correlation of particle count to sample time, the double sampling estimates of mean time are more precise than single

phase estimates! This clearly demonstrates the potential precision gains through incorporation of a double sampling approach.

CWD sampling efficiency may also be increased through the use of remote sensing based methods. Airborne laser scanner data, for example, has provided researchers with forest characteristic data over large areas for a relatively low cost (Nelson *et al*. 2004; Pesonen *et al*. 2009). In Delaware, airborne laser profiling was used in conjunction with LIS to successfully estimate biomass and carbon. In less than two days, a light detecting and ranging (LIDAR) system collected data for approximately 1300 $km^2$ of forest, at a cost of only $6000 (Nelson *et al*. 2004). This information can be used to more effectively sample large areas by strategically allocating sampling efforts (Pesonen *et al*. 2009), or by providing auxiliary data for double sampling applications.

Other novel sampling methods are frequently being introduced, several of which provide precise and cost effective estimates of CWD attributes. Sampling methods that could provide more efficient alternatives to LIS include transect relascope, point relascope (Gove *et al*. 1999), perpendicular distance (Williams & Gove 2003), line intersect distance (Affleck 2008) sampling, and others. However, in order to most efficiently estimate carbon on a global scale, harmonization of sampling techniques must be addressed promptly. Implementation of "comparable" methods requires critical investigation of sampling designs, methods, and estimators to facilitate compilation of carbon data internationally. Efficient and precise strategies must be published widely, for further investigation in various forest types before international integration of carbon budgets is achieved.

# 4. SUMMARY & CONCLUSIONS

Throughout the various stages of decay, CWD provides habitat for many plant and wildlife species (Hutto 1995, 2006; Bowman *et al*. 2000) and adds structural diversity to aquatic and terrestrial systems (Harmon *et al*. 1989; Thomas 1979). Essential soil nutrients are extracted from the soil during vegetative growth, and are returned to the soil as organic material decomposes (Keane 2008a). The inherent carbon storage property of CWD makes retention an appealing option for sequestration. However, overabundance of CWD may contribute to excessive fire hazard, and must be managed appropriately (Brown *et al*. 2003).

As climate change and global carbon inventories become increasingly important, effective CWD assesment becomes crucial. In order to properly inventory and track changes in this resource, we must develop more precise estimators, while maintaining an efficient and feasible sampling design (Woldendorp *et. al.* 2004; Woodall *et al*. 2008). Applying double sampling to current CWD sampling strategies may provide a means for increasing precision while reducing sampling costs. However, despite the correlation of both aggregate volume and abundance to aggregate length, the cost savings from double sampling do not offset the loss in precision associated with smaller sample sizes and regression estimates. Other auxiliary variables that are more strongly correlated to the variable of interest, or a less expensive yet informative method of phase 1 sampling may warrant the application of double sampling to LIS.

# 5. REFERENCES


Affleck, D.L.R. 2008. A line intersect distance sampling strategy for downed wood inventory. *Canadian Journal of Forest Research*. 38: 2262-2273.

Agee, J.K. 1993. Fire Ecology of Pacific Northwest Forests. Island Press, Covelo, California.

Albini, F.A., and E.D. Reinhardt. 1995. Modeling ignition and burning rate of large woody natural fuels. *International Journal of Wildland Fire* 5(2):81 91.

Baker, T. R., Phillips, O. L., Malhi, Y. Almeidas, S, Arroyo, L., DiFiore, A., Erwin, T, Killeen, T.J., Laurance, S.G., Laurance, W.F., Lewis, S.L., Lloyd, J. Monteagudoss, A., Neill, D.A., Patino, S., Pitman, N.C.A, Silva, J.N.M, and R.V. Martinez. 2004. Variation in wood density determines spatial patterns in Amazonian forest biomass. *Global Change Biology* **10**(5): 545-562.

Bowman, J.C, Sleep, D., Forbes, G.J., and M. Edwards. 2000. The association of small mammals with coarse woody debris at log and stand scales. *Forest Ecology and Management* 129:119-124.

Brown, J.K., 1974. Handbook for Inventorying Downed Woody Material. GTR-INT-16, USDA Forest Service, Ogden, UT.

Brown, S. 2002. Measuring carbon in forests: current status and future challenges. *Environmental Pollution* **116**(3): 363-372.

Brown, J. K., Reinhardt, E.D. and K.A. Kramer. 2003. Coarse woody debris: managing benefits and fire hazard in the recovering forest. Gen. Tech. Rep. RMRS GTR- 105. Ogden, UT: U.S. Department of Agriculture, Forest Service, Rocky Mountain Research Station. 16 p.

Bull, E. L. and R. S. Holthausen. 1993. Habitat use and management of pileated woodpeckers in northeastern Oregon. *Journal of Wildlife Management* **57**(2): 335-345.

Canfield, R. H. 1941. Application of the line intercept method in sampling range vegetation. *Journal of Forestry* **39**: 388-394.

Carey, A. B. and M. L. Johnson. 1995. Small mammals in managed, naturally young, and old-growth forests. *Ecological Applications* **5**(2): 336-352.

Cornwell, W. K., Cornelissen, J. H. C., Allison, S.D., Bauhus, J., Eggleton, P., Preston, C.M., Scarff, F., Weedon, J.T., Wirth, C., and A.E. Zanne. 2009. Plant traits and wood fates across the globe: rotted, burned, or consumed? *Global Change Biology* **15**(10): 2431-2449.

Covington, W. W. and S. S. Sackett. 1984. The effect of a prescribed burn in southwestern ponderosa pine on organic-matter and nutrients in woody debris and forest floor. *Forest Science* **30**(1): 183-192.

Dellenbaugh, M., Ducey, M. J.and J.C. Innes. 2007. Double sampling may improve the efficiency of litterfall estimates. *Canadian Journal of Forest Research* **37**(4): 840-845.

DeVries, P.G. 1973. A general theory on line-intersect sampling with application to logging residue inventory. Mededdlingen Landbouw Hogeschool No. 73–11, Wageningen, The Netherlands, 23 pp.

DeVries, P. G. 1974. Multistage line intersect sampling. *Forest Science* **20**(2): 129-133.

Fauconnier, C. and G. Haesbroeck. 2009. Outliers detection with the minimum covariance determinant estimator in practice. Statistical Methodology. **6**:363-379.

Franklin J.F., Shugart, H.H. and M.E. Harmon. 1987. Tree death as an ecological process. *BioScience* 37:550–6.

Fule, P. Z. and W. W. Covington. 1994. Double sampling increases the efficiency of forest floor inventories for Arizona ponderosa pine forests. *International Journal of Wildland Fire* **4**(1): 3-10.

Gove, J. H., Ringvall, A., Stahl, G. and M.J. Ducey. 1999. Point relascope sampling of downed coarse woody debris." *Canadian Journal of Forest Research* **29**(11): 1718-1726.

Gregoire T. G. and N. S. Monkevich 1994. The Reflection Method of Line Intercept Sampling to Eliminate Boundary Bias." *Environmental and Ecological Statistics* 1: 219.

Gregoire T.G. and H.T. Valentine. 2008. *Sampling Strategies for Natural Resources and the Environment*. Chapman and Hall, CRC.

Harmon, M.E., Franklin, J.F., Swanson, F.J., Sollins, P., Gregory, .V., Lattin, J.D., Anderson, N.H., Cline, S.P., Aumen, N.G., Sedell, J.R., Lienkaemper, G.W., Cromack Jr., K. and K.W.Cummins. 1986. Ecology of coarse woody debris in temperate ecosystems. Advanced Ecological Research. 15, 133–302.

Horvitz, D. G. and D. J. Thompson. 1952. A generalization of sampling without replacement from a finite universe. *Journal of the American Statistical Association* **47**, 663-685

Hutto, R.L. 2006. Toward meaningful snag-management guidelines for postfire salvage logging in North American conifer forests. *Conservation Biology*. 20(4): 984-993.

Hutto, R.L. 1995. Composition of bird communities following stand replacement fires in northern Rocky mountain conifer forests. *Conservation Biology*. 9(5): 1041-1058.

Kaiser, L. 1983. Unbiased estimation in line-intercept sampling. *Biometrics* **39**(4): 965-976.

Kashian, D. M., Romme, W. H., Tinker, D.B., Turner, M.G. and M.G. Ryan. 2006. Carbon storage on landscapes with stand-replacing fires. *Bioscience* **56**(7): 598-606.

Keane, R.E. 2008a. Surface fuel litterfall and decomposition in the northern Rocky Mountains, U.S.A. Research Paper RMRS-RP-70. Fort Collins, CO: U.S. Department of Agriculture, Forest Service, Rocky Mountain Research Station. 22 p.

Keane, R.E. 2008b. Biophysical controls on surface fuel litterfall and decomposition in the northern Rocky Mountains, U.S.A. *Canadian Journal Forest Research*. 38:1431-1445.

Klutsch, J. G., J. F. Negron, Costello, S.L, Rhoades, C.C., West, D.R., Popp, J., and R. Caissie. 2009. Stand characteristics and downed woody debris accumulations associated with a mountain pine beetle (*Dendroctonus ponderosae* Hopkins) outbreak in Colorado. *Forest Ecology and Management* **258**(5): 641-649.

MacNally, R., Parkinson, A. Horrocks, G. Conole, L. and C. Tzaros. 2001. Relationships between terrestrial vertebrate diversity, abundance and availability of coarse woody debris on south-eastern Australian floodplains. *Biological Conservation* **99**(2): 191-205.

Manning, T. and P. Chytyk. 2008. Mountain pine beetle infestation: coarse woody debris and impacts on furbearers. Ministry of Environment Mountain Pine Beetle Action Team (MPBAT) by Manning, Cooper and Associates Ltd., Victoria, B.C. pp12.

Mandallaz, D. and R. H. Ye 1999. Forest inventory with optimal two-phase two-stage sampling schemes based on the anticipated variance. *Canadian Journal of Forest Research* **29**(11): 1691-1708.

McCay, T.S. 2000. Use of woody debris by cotton mice (*Peromyscus gossypinus*) in a southeastern pine forest. Journal of Mammology, **81**(2):527-535.

McKenny, H.C., Keeton, W.S., and T.M Donovan. 2006. Effects of structural complexity enhancement on eastern red-backed salamander (*Plethodon cinereus*) populations in northern hardwood forests. *Forest Ecology and Management*. 230:186-196.

Metzger, K. L., E. Smithwick, A. H., Tinker, D.B., Rommec, W.H., Balser, T.C. and M.G. Turner. 2008. Influence of coarse wood and pine saplings on nitrogen mineralization and microbial communities in young post-fire *Pinus contorta*. *Forest Ecology and Management* **256**(1-2): 59-67.

Monsanto, P.G. and J.K. Agee. 2008. Long term post fire dynamics of coarse woody debris after salvage logging and implications for soil heating in dry forests of the eastern Cascades, Washington. *Forest Ecology and Management*. 255:3952-3961.

Nelson, R. Short, A. and M. Valenti. 2004. Measuring biomass and carbon in Delaware using and airborne profiling LIDAR. *Scandinavian Journal of Forest Research* 19: 500-511

Nemec, A.F.L., and G. Davis. 2002. Efficiency of six line intersect sampling designs for estimating volume and density of coarse woody debris. Res. Sec., Van. For. Reg., B.C. Min. For., Nanaimo, B.C. Tec. Rep.TR-021/2002.

Ott, R.L. and M. Longnecker. 2001. An introduction to statistical methods and data analysis. Fifth edition. Thompson Learning Inc.

Owens, A. K., Moseley, K. R., McCay, T.S., Castleberry, S.B., Kilgo, J.C. and W.M. Ford. 2008. Amphibian and reptile community response to coarse woody debris manipulations in upland loblolly pine (*Pinus taeda*) forests. *Forest Ecology and Management* **256**(12): 2078-2083.

Pesonen, A., Leino, O., Maltmo, M. and A. Kangas. 2009. Comparison of field sampling methods for assessing coarse woody debris and use of airborne laser scanning as auxiliary information. *Forest Ecology and Management* **257**(6): 1532-1541.

Reinhardt, E.D., Keane, R.H., and J.K. Brown. 1997. First order fire effects model: FOFEM 4.0 User's guide. USDA For. Serv. Gen. Tech Rep. INT-GTR-344 p.65.

Ringvall, A. and G. Stahl. 1999. Field aspects of line intersect sampling for assessing coarse woody debris. *Forest Ecology and Management.* **119:** 163-170.

Rogers, G.F. and J. Steele. 1980. Sonoran desert fire ecology. USDA Forest Serv. Gen. Tech. Rep. RM-81.

Rousseeuw, P.J. and A.M. Leroy. 1987. Robust regression and outlier detection. New York: John Wiley.

Shiver, B.D. and Borders, B.E. 1996. Sampling Techniques for Forest Resource Inventory, John Wiley and Sons Inc.

Sikkink, P. G. and R. E. Keane. 2008. A comparison of five sampling techniques to estimate surface fuel loading in montane forests. *International Journal of Wildland Fire* **17**(3): 363-379.

Spetich, M. A., Shifley, S. R. and G.R. Parker. 1999. Regional distribution and dynamics of coarse woody debris in midwestern old-growth forests. *Forest Science* **45**(2): 302-313.

Stevens, V. 1997. The ecological role of coarse woody debris: an overview of the ecological importance of CWD in B.C. forests. Research Brochure, B.C. Ministry of Forestry., Victoria, B.C. Work. pp. 30

Stevenson, S. K., Jull, M. J. and B.J. Rogers. 2006. Abundance and attributes of wildlife trees and coarse woody debris at three silvicultural systems study areas in the Interior Cedar-Hemlock Zone, British Columbia. *Forest Ecology and Management* **233**(1): 176-191.

Thomas, J.W. 1979. Wildlife habitats in managed forests, the Blue Mountains of Oregon and Washington. USDA Forest Service Agricultural Handbook. 553. Washington Office. Washington D.C.

Thompson, S.K. 2002. Sampling Second Edition. New York: J. Wiley & Sons.

Tinker, D.B. and D.H. Knight. 2000. Coarse woody debris following fire and logging in Wyoming lodgepole pine forests. *Ecosystems* **3**(5):472–483.

Todd, B.D., Luhring, T.M., Rothermel, B.B. and J.W. Gibbons. 2009. Effects of forest removal on amphibian migrations: implications for habitat and landscape connectivity. *Journal of Applied Ecology* **46**(3): 554-561.

Ulyshen, M.D., Hanula, J.L., Horn. S., Kilgo, J.C. and C.E. Moorman. 2004. Spatial and temporal patterns of beetles associated with coarse woody debris in managed bottomland hardwood forests. *Forest Ecology and Management* **199**(2-3): 259-272.

Warren, W.G. and P.F. Olsen. 1964. A line-intersect technique for assessing logging waste. *Forest Science*. 10, 267–276.

Williams, M.S. and J.H. Gove. 2003. Perpendicular distance sampling: an alternative method for sampling downed coarse woody debris. *Can. J. For. Res.* **33** 1564 – 1579.

Woldendorp G., Keenan, R.J., Barry, S. and R.D. Spencer. 2004. Analysis of sampling methods for coarse woody debris. *Forest Ecology and Management.* 198: 16.

Woodall, C.W., Charney, J.J., Liknes, G.C. and B.E. Potter. 2005. What is the fire danger now? Linking fuel inventories with atmospheric data. *Journal of Forestry* **103**(6): 293-298.

Woodall, C.W., Heath, L.S. and J.E. Smith. 2008. National inventories of down and dead woody material forest carbon stocks in the United States: Challenges and opportunities. *Forest Ecology and Management* **256**(3): 221-228.

Woodall C.W. and G.C Liknes 2008. Relationships between forest fine and coarse woody debris carbon stocks across latitudinal gradients in the United States as an indicator of climate change effects. *Ecological Indicators* **8**: 686-690.

Woodall, C.W., Rondeux, J., Verkerk, P.J. and G. Stahl. 2009. Estimating dead wood during national forest inventories: a review of inventory methodologies and suggestions for harmonization. *Environmental Management* **44**(4): 624-631.

Zielonka, T. and G. Piatek. 2004. The herb and dwarf shrubs colonization of decaying logs in subalpine forest in the Polish Tatra Mountains. *Plant Ecology*. 173:63-72.